

REVIEW

Tractometry of Human Visual White Matter Pathways in Health and Disease

Hiromasa Takemura^{1,2,3*} , John A. Kruper⁴ , Toshikazu Miyata^{1,3} ,
and Ariel Rokem⁴ 

Diffusion-weighted MRI (dMRI) provides a unique non-invasive view of human brain tissue properties. The present review article focuses on tractometry analysis methods that use dMRI to assess the properties of brain tissue within the long-range connections comprising brain networks. We focus specifically on the major white matter tracts that convey visual information. These connections are particularly important because vision provides rich information from the environment that supports a large range of daily life activities. Many of the diseases of the visual system are associated with advanced aging, and tractometry of the visual system is particularly important in the modern aging society. We provide an overview of the tractometry analysis pipeline, which includes a primer on dMRI data acquisition, voxelwise model fitting, tractography, recognition of white matter tracts, and calculation of tract tissue property profiles. We then review dMRI-based methods for analyzing visual white matter tracts: the optic nerve, optic tract, optic radiation, forceps major, and vertical occipital fasciculus. For each tract, we review background anatomical knowledge together with recent findings in tractometry studies on these tracts and their properties in relation to visual function and disease. Overall, we find that measurements of the brain's visual white matter are sensitive to a range of disorders and correlate with perceptual abilities. We highlight new and promising analysis methods, as well as some of the current barriers to progress toward integration of these methods into clinical practice. These barriers, such as variability in measurements between protocols and instruments, are targets for future development.

Keywords: *diffusion magnetic resonance imaging, tractography, tractometry, vision, white matter*

Neuroimaging Measurements of Brain White Matter

Vision is a crucial sensory system for humans to support daily life, and a loss of visual function significantly reduces the quality of life.¹ For this reason, understanding the health and disease of the visual system is a major goal of biomedical

research, including structural neuroimaging using MRI.² This review focuses specifically on one component of the visual system: its white matter connections. It provides a brief overview of current neuroimaging data acquisition and analysis methods for analyzing white matter (sections “MRI Measurements of Brain White Matter” and “Tractometry Methods”), with an emphasis on their applications to understanding major early visual white matter pathways in health and disease (section “Tractometry of Early Visual White Matter Tracts”). Additionally, this review discusses remaining open questions and future prospects (section “Future Perspectives and Open Questions”).

According to recent estimates, the brain contains approximately 85 billion nerve cells (neurons).³ Large assemblies of neurons form networks that rapidly distribute information across the brain and integrate it, supporting the range of flexible behaviors exhibited by humans. The brain is composed of gray matter, which consists of cell bodies of neurons, and white matter, which consists of the myelinated axons of the neurons. Myelin plays an important role in information transmission because it increases the speed of communication between neurons as well as its fidelity.⁴

¹Division of Sensory and Cognitive Brain Mapping, Department of System Neuroscience, National Institute for Physiological Sciences, Okazaki, Aichi, Japan

²Graduate Institute for Advanced Studies, SOKENDAI, Hayama, Kanagawa, Japan

³Center for Information and Neural Networks (CiNet), Advanced ICT Research Institute, National Institute of Information and Communications Technology, Suita, Osaka, Japan

⁴Department of Psychology and eScience Institute, University of Washington, Seattle, WA, USA

*Corresponding author: Division of Sensory and Cognitive Brain Mapping, Department of System Neuroscience, National Institute for Physiological Sciences, 38 Nishigonaka Myodaiji, Okazaki, Aichi 444-8585, Japan.
E-mail: htakemur@nips.ac.jp



This work is licensed under a Creative Commons Attribution-NonCommercial-NoDerivatives International License.

©2024 Japanese Society for Magnetic Resonance in Medicine

Received: January 23, 2024 | Accepted: May 1, 2024

Myelination proceeds through a prescribed developmental program, with a progression of myelination in different regions through infancy, childhood, and adolescence.^{5,6} At the same time, myelination is also activity-dependent: the glial cells (oligodendrocytes) that constitute the myelin sheath around neuronal axons respond to electrical activity in the neurons, preferentially myelinating electrically active axons.^{7–13} Furthermore, properties of brain connections, such as their level of myelination, can adapt to external stimuli, exhibit plasticity induced by learning, and are sensitive to brain disease.^{14–16} Injury to these connections can lead to significant brain dysfunction, resulting in neurological, psychiatric, and neurodevelopmental syndromes.¹⁷ For these reasons, understanding the white matter is essential for a complete understanding of development, learning, and a range of different neurological and mental health disorders.

MRI plays an essential role in investigating the involvement of the brain white matter in adaptive and flexible behavior, and the application of MRI to a range of brain diseases is already making some headway into clinical applications as well. The present review focuses on measurements of the parts of the white matter that transmit visual signals to the brain. We focus specifically on non-invasive measurements that use diffusion-weighted MRI (dMRI) to delineate the trajectory of the visual white matter pathways and to quantify tissue properties along these pathways.^{18–22} In the following sections, we will introduce methods of white matter quantification from dMRI data and methods for the delineation of specific white matter pathways. After this methodological introduction, we will review findings about the visual pathways following the progression of visual information through the brain from the retina through the optic nerve and optic tract to the thalamus and from there onwards through the optic radiations that connect the thalamus and visual cortex. We will then review findings about cortico-cortical visual pathways: the vertical occipital fasciculus (VOF), which connects the dorsal and ventral portions of the visual cortex, and the posterior callosal connection (forceps major), which connects the visual cortex in both hemispheres.

dMRI is the only currently available method to measure the trajectory of white matter connections *in vivo*. It relies on a pulsed-gradient spin echo (PGSE) sequence to sensitize the MRI measurements to diffusion in many different directions in every location in the brain, with increased signal loss in locations and directions where the average diffusion distance of water molecules is larger. The inverse relationship between diffusivity and signal in the PGSE experiment was first discovered and mathematically defined by Stejskal and Tanner and is known as the Stejskal–Tanner equation.²³ In accordance with this equation, in places where diffusion is restricted by white matter components, such as the membranes of the axonal nerve fibers and myelin sheaths surrounding them (Fig. 1A, B, and C), the signal varies across different measurement directions (Fig. 1D and E). The signal parallel to the nerve fibers is relatively decreased, indicating

a large average distance of diffusion of water molecules (schematized as blue circles in Fig. 1C), while measurements orthogonal to the fibers indicate a smaller degree of diffusivity (Fig. 1D, E, and F). These differences can be used to estimate the location and direction of large nerve fiber bundles through the white matter and other properties of the white matter tissue within the measurement voxel. While the volume of the measurement voxels in dMRI is usually on the order of a few mm³, the PGSE sequence sensitizes the MRI signal to the motion of water on the scale of a few microns. For example, it is sensitive to their restriction within axonal compartments (Fig. 1C3 and 1C4), or between tightly packed highly myelinated axons (Fig. 1C2). This means that the measurement is also highly sensitive to the microstructure of brain white matter tissue. In tandem with other quantitative MRI methods, estimates of brain white matter microstructure can be used to assess the physical properties of brain connection in the living human brain at millimeter resolution.

One of the first models to derive tissue properties from dMRI data was the diffusion tensor model proposed by Basser and colleagues (1994, 1996)^{24,25} (Fig. 1F). This work was important because it connected the signal measured in dMRI with a model of underlying tissue microstructure. Soon after originally proposing this model, Pierpaoli and Basser (1996) also derived tensor-based scalar quantities that summarize the physical properties of brain tissue in each voxel, such as the mean diffusivity (MD), which is the mean of the eigenvalues of the self-diffusion tensor, and fractional anisotropy (FA), a normalized measure of variance among the eigenvalues.²⁶ These quantities are sensitive to relevant biological tissue characteristics, such as the myelination of white matter, axon density, and geometrical configuration.

While the diffusion tensor model is a good model in terms of its fitting accuracy to dMRI signals and robustness of metrics derived from it (such as MD and FA^{27,28}), it has two major limitations: (1) it cannot represent the crossing of more than one fiber within a voxel and (2) it cannot distinguish dMRI signals from different biological sources, such as signals from water molecules in intracellular or extracellular space. Subsequent research proposed methods that attempt to address these limitations. One fruitful research direction is to acquire dMRI data with a larger number of diffusion gradient orientations and to fit more complex models that better account for crossing fibers in the voxel (Fig. 1G).^{27,29–31} Another parallel research track is to perform measurements using multiple-diffusion weighting values and to fit more sophisticated models that are sensitive to a larger range of physical tissue properties, including properties that are more specifically related to the biological components within the tissue.^{32–36} While these models have their pitfalls,^{37,38} they improved tractography and dMRI-based quantification of white matter tissues.

Models of dMRI, such as the diffusion tensor model, also provide information about the orientations of groups of

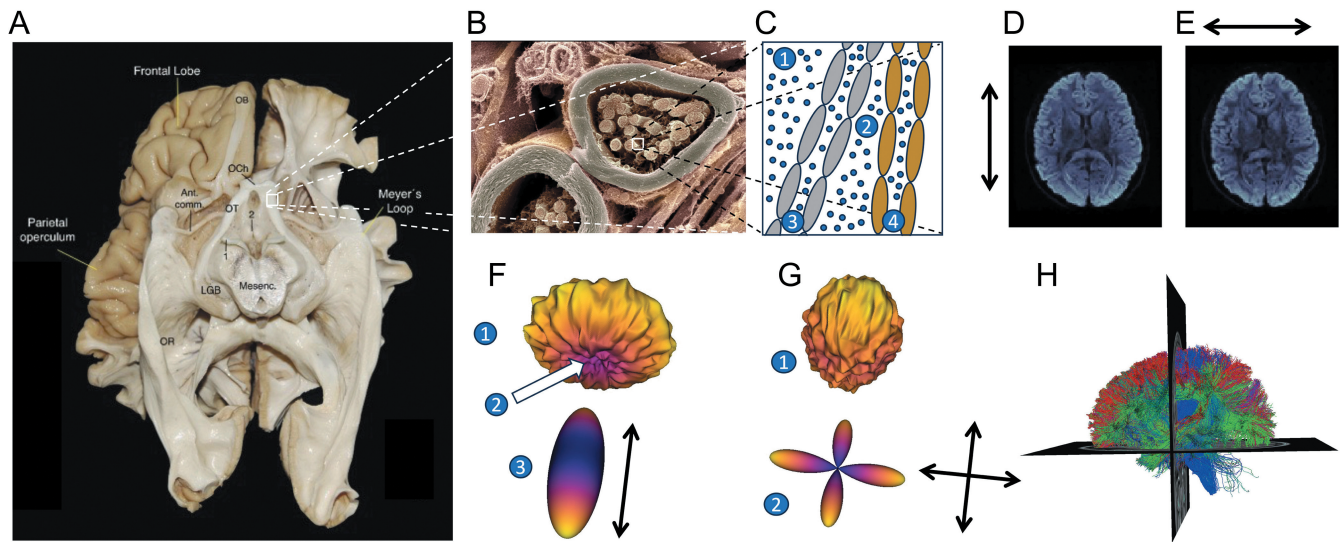


Fig. 1 Measurements of human brain connections with dMRI. **A:** The visual pathways in the human brain organize into large fascicles, here shown in a *post-mortem* dissection (Source: López-Elizalde et al. (2021),²⁷⁵ provided under the Attribution 4.0 International Creative Commons license [CC BY 4.0]). 1: oculomotor nerve, 2: mammillary bodies. **B:** Zooming in on these fascicles, here in a microscopic image of a nerve fiber, we observe that the fascicles are made up of individual myelinated axons (source: Wellcome Collection. <https://wellcomecollection.org/works/ugyj9njv>, Dr. David Furness, provided under the Attribution-NonCommercial 4.0 International Creative Commons license [CC BY-NC 4.0]). **C:** In a schematic diagram of two such axons, the diffusion of different populations of water molecules (small blue circles) is affected by the presence of the tissue in different ways: molecules outside of the bundle (C1) may diffuse freely in all directions, and their diffusion will be governed primarily by temperature and the self-diffusion properties of water. This diffusion is isotropic. Within the bundle, water that is between tightly packed axons (C2) may be affected by the degree of myelination of different axons (e.g., here myelination of two different axons is schematically depicted in gray and brown). Within the axons (C3 and C4), water is affected by the presence of cellular membranes. Moreover, the degree to which water diffusion is anisotropic within a measurement voxel may be affected by the distribution of different axons and their orientations. **D:** A horizontal slice through a PGSE dMRI measurement demonstrates that the signal is sensitized to diffusion in particular directions. Here, the gradient is approximately aligned with the anterior-posterior axis of the brain and the signal is higher in portions of the corpus callosum that are oriented orthogonal to the gradient direction. **E:** When the gradient is oriented along the right-left axis of the brain, the signal is higher in portions of the posterior callosum that are oriented orthogonal to this gradient direction. **F:** Models of the white matter explain the diffusion profile in multiple different directions. Here, the signal is high along multiple directions along the edge of the “donut” shape (F1) and low in some directions around the center of the “donut” (F2). This is consistent with a diffusion tensor model that is oriented along the low signal (F3). **G:** A signal with multiple peaks and valleys (G1) may be more consistent with a model that has multiple directions of crossing fibers, here represented as the fiber orientation distribution function from the CSD model (G2).³¹ **H:** Models such as the tensor and CSD serve as cues for computational tractography algorithms, which generate estimates of white matter fibers. Here, these estimates are represented as three-dimensional curves called “streamlines,” each colored to indicate their average direction: red for left-right, green for anterior-posterior and blue for inferior-superior. Ant. Comm., anterior commissure; dMRI, diffusion-weighted MRI; CSD, constrained spherical deconvolution; LGB, lateral geniculate body (also lateral geniculate nucleus, LGN); Mesenc, mesencephalon; OB, olfactory bulb; OCh, optic chiasm; OR, optic radiation; OT, optic tract; PGSE, pulsed-gradient spin echo.

axons in the white matter. Thus, they are used as cues for computational algorithms for reconstructing white matter pathways from dMRI signals (tractography; Fig. 1H). Tractography algorithms follow the directions of major white matter pathways that are estimated from the pattern of diffusion in each voxel. One of the important evolutions in modeling brain connections comes from the realization that the pattern of dMRI measurements can reflect the presence of more than one direction of brain white matter fibers within a voxel.^{29,39} Models that account for these multiple directions allow computational tractography algorithms to generate crossings of different fibers within each voxel, allowing for a more detailed and accurate representation of the underlying anatomy,^{31,40–42} and of the

measured signal.²⁷ Algorithms for computational tractography take the estimates of directions within individual voxels and connect them to create longer curves (also known as “streamlines,” because some of these methods rely on techniques originally developed in computational fluid dynamics⁴³). There are many different approaches for propagating streamlines through white matter, from deterministic methods proposed in the late 1990s^{44,45} to probabilistic methods that better account for the inherent noise levels of the signal and allow multiple sampling opportunities in each voxel.^{30,46,47} Together with recent approaches for filtering streamlines,^{48–53} probabilistic approaches produce overall more accurate representations of the brain connectome than deterministic approaches. However,

some fundamental challenges persist. For example, none of these methods can currently properly adjudicate between kissing and crossing fibers.^{54,55} While tractography methods overcome some of their limitations, researchers need to capitalize on the strengths of this method while being aware of their weaknesses.

Tractometry Methods

There are many approaches for analyzing dMRI data and understanding brain connections. The present review will focus on one approach that we refer to as *tractometry*. This method focuses on the delineation of major white matter anatomical structures within each individual and the analysis of the biophysical properties of white matter tissue within these anatomical structures. This is an application where dMRI has considerable strength⁵⁶ and is relatively robust to the limitations mentioned above and to variability in processing methods.²⁸ The brain's white matter is composed of large bundles of axons that travel together in fascicle-like structures that are also known as tracts. Many of these tracts were first thoroughly studied using *post-mortem* anatomical methods, and therefore, their positions and trajectories are validated independently. This means that their delineation in dMRI-based tractography is considered well-justified and less prone to false-positive tractography results.⁵⁵ The first part of tractometry analysis focuses on finding the trajectory of these tracts in the individual brain from the results of tractography. Researchers aim to identify white matter tracts by selecting streamlines that satisfy criteria derived from known anatomical information (Fig. 2).⁵⁷ For example, one can select streamlines that reach close to the known cortical endpoints of the tract. Alternatively, one can also select streamlines that pass through waypoint ROIs,⁵⁸ which are defined based on the expected trajectory of the tract (see Table 1 for examples of ROIs used in previous studies). A population-based atlas of the probabilistic locations of the different tracts can provide more information about the expected location of the tract.⁵⁹ Because the estimates of individual streamlines are sensitive to noise, researchers often also use “cleaning” methods on the tract, by removing outlier streamlines whose trajectories deviate from the overall expected shape of the tract.⁵⁷ Once tract locations are identified, the tissue properties along the length of the tracts can be assessed (Fig. 3).

The overall approach has its roots in work from the early 2000s focused on white matter quantification⁶⁰ and the idea of Pointwise Assessment of Streamline Tractography Attributes (PASTA).⁶¹ Subsequent work took a variety of approaches both to the delineation of the different anatomical structures^{62–66} and to the quantification of tissue properties.⁶⁷ While these different methods enable similar tract-specific quantification of tissue properties, they use different strategies for tract segmentation and adopt different types of anatomical prior information.⁶⁸ Providing

recommendations for the best strategy is beyond the scope of this article, since it depends on various factors such as the anatomical pathways that researchers are interested in studying, the types of target populations, and data acquisition parameters. One practical approach to comparing different methods is to evaluate the test–retest reliability that each method offers.²⁸

Locating the tracts at the level of each individual's tractography data both mitigates confounds that arise in spatially smoothed voxel-based morphometry approaches, as well as endowing the measurements with specific anatomical meaning. On the other hand, delineation of tracts based on tractography can be difficult in the presence of brain tumors or lesions.⁶⁹ Nevertheless, studies also show high robustness of tract delineation methods even in the presence of white matter lesions due to multiple sclerosis, while at the same time demonstrating that correspondence with probabilistic maps of tracts is rather low, again highlighting the advantages of individualized tract delineation.⁷⁰

Tractometry of Early Visual White Matter Tracts

Tractometry analysis for visual pathways has several essential aims. First, tract-specific investigation of white matter tissue properties is crucial for evaluating disorders directly affecting white matter, such as optic neuritis.⁷¹ Second, tractometry is important for understanding how disorders that damage photoreceptor cells (such as macular degeneration^{72,73} and retinitis pigmentosa⁷⁴), or that damage retinal ganglion cells (RGCs) and the optic nerve (such as glaucoma⁷⁵), affect subsequent white matter pathways carrying visual signals from the retina to the brain. A better understanding on the effects of specific disorders on the different stages of visual information processing should improve our ability to establish the best intervention strategy for each disorder (e.g., retinal prostheses,^{76,77} cortical prostheses,⁷⁸ or stem cell therapies⁷⁹). Finally, tractometry is important to address neuroscientific questions on how properties of each white matter tract are related to visual functions, such as face recognition.^{21,80}

In this section, we will provide an updated review of the recent progress in recent tractometry studies on major white matter tracts in the visual system. While a previous review²¹ focused on how dMRI studies on the white matter help us understand the neural basis of perception and functional organization of the visual cortex, the present review article focuses on how the tractometry approach helps us understand early visual white matter tracts in relation to visual disorders, such as common retinal diseases (see^{81–84} for reviews on white matter tracts in the temporal, frontal, and parietal cortex that support higher visual functions and see Hanekamp et al.⁸⁵ for a study investigating the impact on glaucoma in white matter tracts outside the occipital lobe). We will also provide reviews on recent developments in

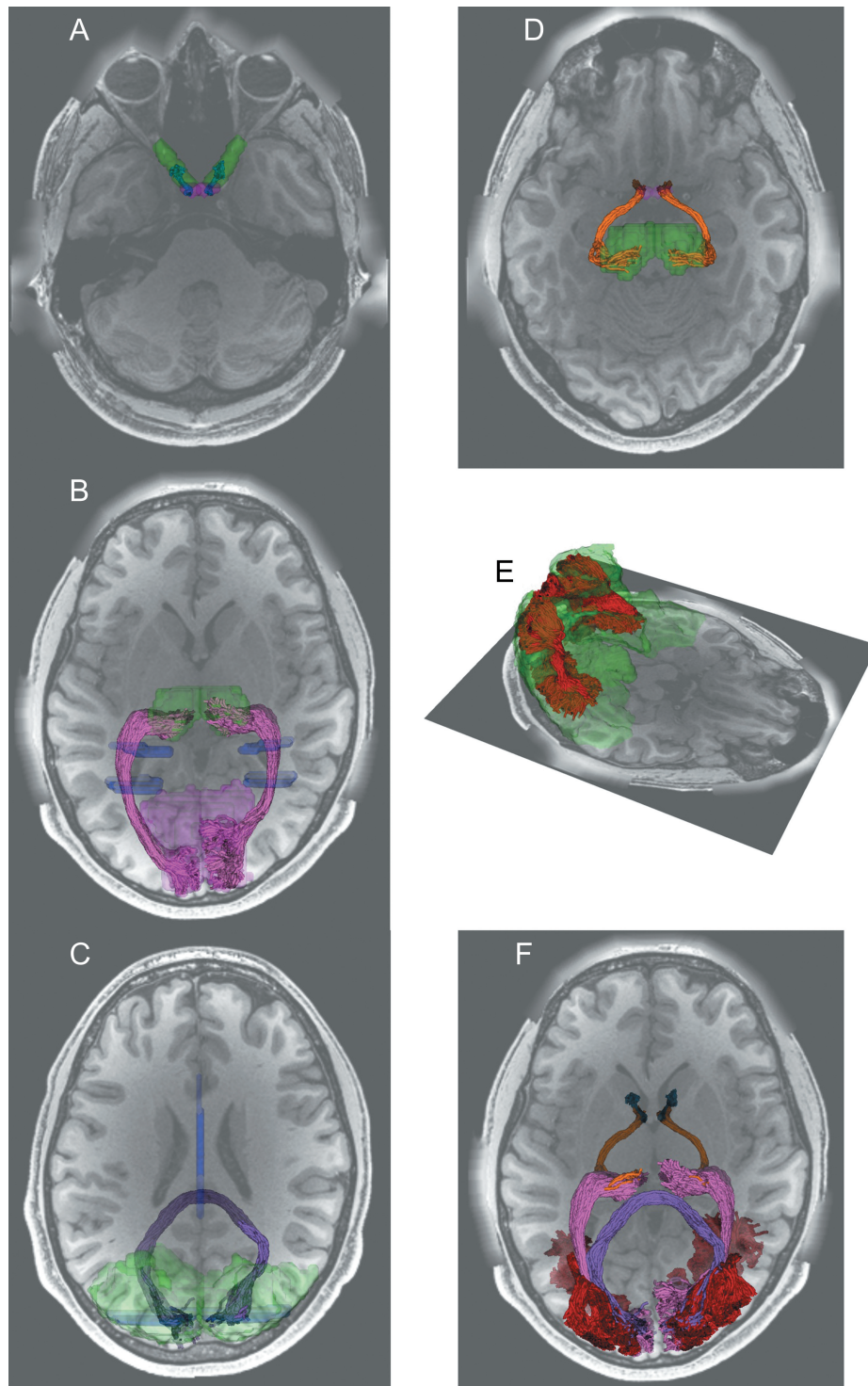


Fig. 2 Visual white matter tracts were identified by tractography in dMRI data from representative participants in the Human Connectome Project Young Adult data.²⁵⁰ **A:** The optic nerve (blue) was identified by tractography and mask ROIs (green) generated by automated segmentation of a structural image.¹⁰⁶ The optic nerve and the optic chiasm (purple) were overlaid on an axial section of a T1-weighted image. **B:** The optic radiation (magenta) was identified using waypoint ROIs (blue) and endpoint ROIs (thalamus, green; primary visual cortex, light purple) transformed from the Montreal Neurological Institute (MNI) template space.¹⁸² **C:** The forceps major (dark purple) was identified from a waypoint ROI (blue) in the corpus callosum and endpoint ROIs (green) in the occipital cortex of each hemisphere. **D:** The optic tract (orange) was identified by using the optic chiasm (purple) and the thalamus (green) identified by segmentation on structural images as endpoint ROIs. **E:** The vertical occipital fasciculus (red) was identified by using dorsal and ventral visual areas (green) identified by using the automated anatomical labeling atlas.²⁷⁶ **F:** All identified tracts were overlaid on an axial section of a T1-weighted image.

Table 1 ROIs used for identifying visual white matter pathways using tractography in previous studies

Tract	ROIs	Reference
ON	Optic nerve head (manually placed sphere) and optic chiasm (FreeSurfer segmentation ¹¹⁴ on structural image).	Miller et al., 2019 ¹⁰⁸ ; Takemura et al., 2023 ¹⁰⁵
OT	Optic chiasm (FreeSurfer segmentation on structural image) and LGN (manually placed sphere on structural image with a guide of deterministic tractography from the optic chiasm).	Ogawa et al., 2014 ¹¹⁸ ; Takemura et al., 2019 ¹¹⁹ ; Ogawa et al., 2022 ¹³⁰
	Optic chiasm (nonlinear warping from the optic chiasm identified from 5 subjects) and LGN (automated identification from tractography and shape analysis).	Kammen et al., 2016 ¹²⁰
OR	LGN (manually placed sphere with a guide of deterministic tractography from the optic chiasm) and V1 (manually drawn calcarine sulcus).	Sherbondy et al., 2008 ¹¹⁷
	LGN (manually drawn based on structural image with a guide of deterministic tractography from the optic chiasm) and V1 (FreeSurfer segmentation on structural image).	Ogawa et al., 2014 ¹¹⁸ ; Takemura et al., 2019 ¹¹⁹ ; Ogawa et al., 2022 ¹³⁰
	Manually placed NOT ROIs around the medial, anterior, and lateral Mayer's loop.	Chamberland et al., 2017 ¹⁵⁴
	LGN (automated identification from tractography and shape analysis) and V1 (Benson atlas). ^{174,175}	Kammen et al., 2016 ¹²⁰
	Thalamus and V1 (FreeSurfer segmentation on structural image) combined with qT1.	Schurr et al., 2018 ¹⁵⁷
	Thalamus and visual cortex endpoint ROIs and axial waypoint ROIs transformed from the MNI template.	Caffarra et al., 2021 ¹⁸²
	LGN (FreeSurfer-based segmentation) and V1 (Benson atlas). ^{174,175}	Lerma-Usabiaga et al., 2023 ¹²³
Forceps Major	Splenium and occipital lobe white matter.	Dougherty et al., 2005 ¹⁹³
	Coronal waypoint ROIs in each hemisphere's occipital cortex transformed from the MNI space.	Yeatman et al., 2012 ⁵⁷
	Splenium the entire coronal section posterior to the splenium	Scherf et al., 2014 ¹⁹⁵
VOF	Ventral occipitotemporal cortex (FreeSurfer segmentation). In addition, streamlines intermingle with the arcuate fasciculus identified by using the AFQ ⁵⁷ is removed.	Yeatman et al., 2014 ¹⁶⁰
	Waypoint ROIs in the dorsal and lateral part of the occipital white matter.	Takemura et al., 2016 ²⁰⁷
	ROIs used in Yeatman et al., 2014 ¹⁶⁰ and Takemura et al., 2016 ²⁰⁷ combined with qT1.	Schurr et al., 2019 ²¹⁷

LGN; lateral geniculate nucleus, ON, optic nerve; OR, optic radiation; OT, optic tract; qT1, quantitative T1; VOF, vertical occipital fasciculus; V1, primary visual cortex.

dmRI data acquisition, improved tractography algorithms, findings on relatively neglected tracts, and advanced statistical methods for analyzing tractometry data. Short-range white matter pathways in the visual system⁸⁶⁻⁸⁷ are out of the scope of the present review since these pathways are still very challenging to delineate with the existing technology; at

this point, the number of tractometry studies focusing on short-range pathways in the visual system remains limited.

Below, we will review the anatomy of each white matter tract in the visual system, discuss challenges for measurement of each tract, and review previous studies that have utilized the tractometry approach on each tract.

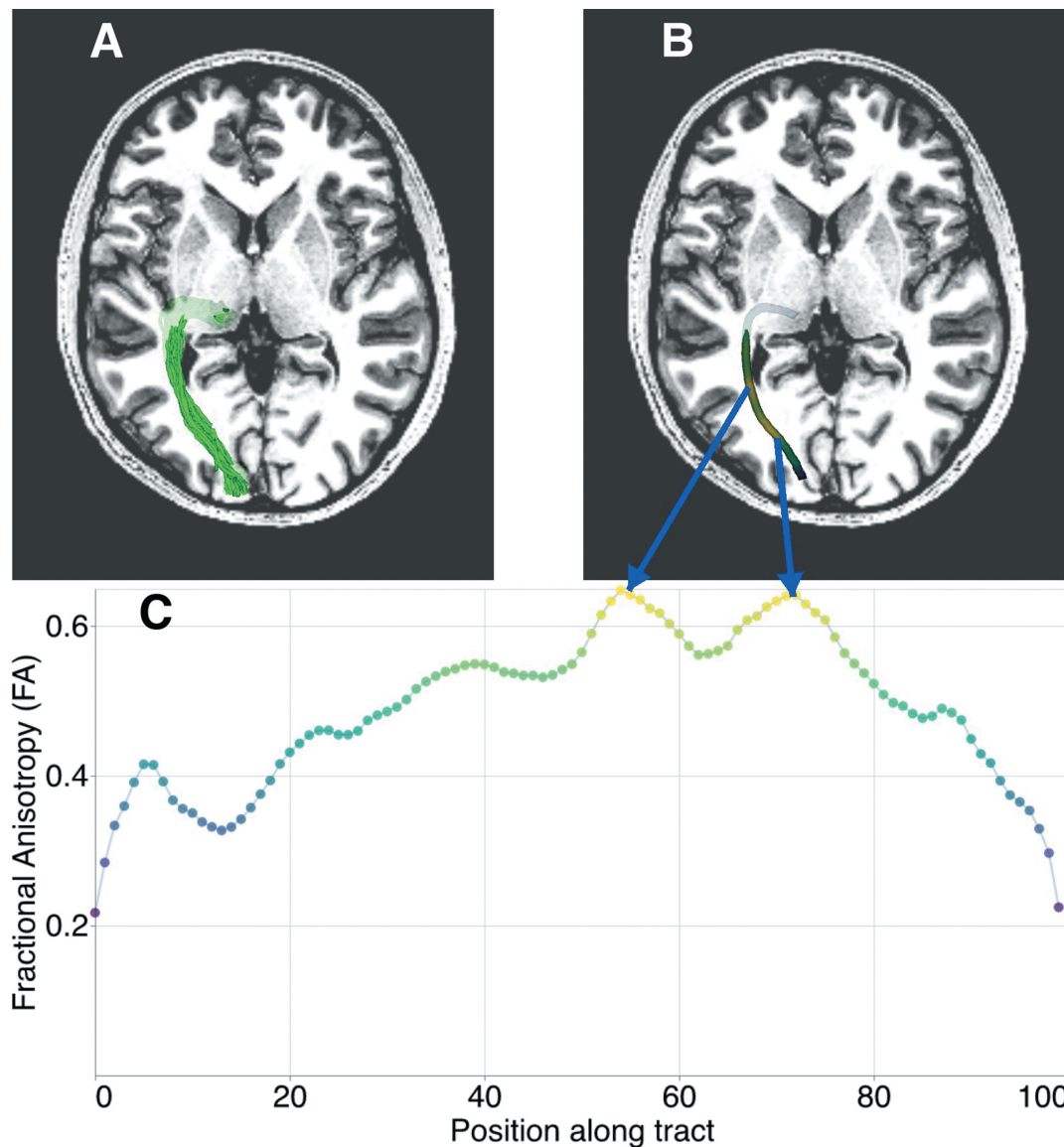


Fig. 3 Tractometry of tissue properties along the length of a white matter tract. **A:** Representation of a white matter tract (here the optic radiation) as streamlines overlaid on an axial section of a T1-weighted image in a randomly selected subject from the Healthy Brain Network^{252,253} dataset. **B:** Individual streamlines are used to sample the volume of tissue properties mapped throughout the brain. The core of the bundle of streamlines, represented as a thick tube, is colored based on values aggregated across the streamlines and weighted based on how closely they resemble the central tendency of the collection of streamlines. **C:** The tract profile is sampled at 100 points along the core of the tract and represented as a one-dimensional vector of values that are used for subsequent analysis and interpretation. The horizontal axis represents position along the tract (left, anterior; right, posterior), whereas the vertical axis represents FA. FA, fractional anisotropy.

Optic nerve

Anatomy

The optic nerve (ON) is a white matter tract composed of axons from RGCs that leave the retina at the optic disk. The left and right ON carry visual signals from the left and right eyes, respectively, from both the left and the right visual fields. The ON continues to the optic chiasm, where some axons from the left and right eyes cross the midline to merge

with uncrossed axons from the contralateral eyes. The ON is an important target for clinical studies on disorders like optic neuritis and glaucoma, which are known to damage this pathway.

Technical considerations

In general, the ON is relatively difficult to measure by dMRI, because of susceptibility-induced artifacts. That is, dMRI images near the optic nerve are typically heavily

distorted and relatively difficult to interpret, because of imaging artifacts derived from the inhomogeneity of the magnetic field in this area, because the ON is located near the paranasal sinus. While it is possible to mitigate these artifacts using distortion correction techniques,⁸⁸ the development of appropriate methods for tractography reconstruction of the ON is still an area of active research.^{89–91}

DMRI measurements of the ON are generally challenging, but there is room for improving them using acquisition strategies that are different from the conventional single-shot echo planar imaging (EPI) that cover the whole brain. One approach is to use a reduced FOV to achieve better measurement quality.^{92–95} While this approach has been used to evaluate the tissue changes of the optic nerve caused by optic neuritis,⁹⁶ a disadvantage of this approach is that it is not possible to evaluate the ON together with other tracts because of the limited FOV available for dMRI measurements. Readout-segmented EPI (rsEPI) has also been proposed to reduce susceptibility-induced image distortion,⁹⁷ while maintaining the whole-brain coverage of dMRI measurement. Several studies demonstrated that rsEPI provides superior image quality of dMRI measurements in the ON, compared with those acquired using a conventional single-shot EPI.^{98–103} The drawback of this method is its prolonged acquisition time, which limits applicability to studies of clinical populations. Simultaneous multi-slice rsEPI¹⁰⁴ has been proposed to mitigate this limitation, and recent work demonstrated that it reduces image distortion of dMRI measurements of the ON and, therefore, reduces the impact of image blurring caused by distortion correction procedures on tractometry results.¹⁰⁵ Lastly, a recently developed automatic segmentation tool uses a convolutional neural network¹⁰⁶ to delineate the likely extent of the ON from structural MRI. The output of this tool can be used as a mask for tractography, which can be used to reconstruct a part of the ON from dMRI data acquired by single-shot EPI, as demonstrated in Fig. 2A.

Tractometry studies on this tract

Because of the aforementioned measurement challenges, tractography of the ON is not very common and many studies focus on visual inspection or use a manually drawn ROI approach¹⁰⁷ to analyze the ON. However, Miller and colleagues (2019)¹⁰⁸ used the tractometry approach to demonstrate a significant FA difference between advanced and mild glaucomatous ON (Fig. 4A), and these measurements are also correlated with clinical measurements of glaucoma, such as retinal nerve fiber thickness and visual field measurements. In addition, Haykal and colleagues (2020)¹⁰⁹ demonstrated that dMRI data acquired from glaucoma patients exhibited abnormalities, such as reduced FA, in the optic nerve. Hong and colleagues (2022)¹¹⁰ used a similar tractometry approach on dMRI data acquired from patients with optic atrophy and demonstrated that diffusivity

measurements, such as FA, were significantly different from atrophic and non-affected ONs. Moon and colleagues (2021)¹¹¹ used the same approach to test cognitively normal elderly populations and demonstrated a correlation between ON tractometry measurements and participants' age. Taken together, although the dMRI-based tractometry approach for the ON has not fully technically matured, there is an increasing number of studies demonstrating its utility to evaluate disease-related changes in this pathway.

Optic tract

Anatomy

The optic tract (OT) is the white matter tract, which connects the optic chiasm and the lateral geniculate nucleus (LGN). In both humans and non-human primates, approximately half of the axons cross over to the opposite hemisphere. In each hemisphere, the OT carries visual information from the opposite side of the visual field. The OT is also an essential target for clinical neuroimaging studies on visual disorders, such as glaucoma, since it carries axons from RGCs, and understanding how disease affects OT microstructure is of high importance. Since axons within the OT continue from the ON, damages to RGCs are likely to affect both the ON and OT. While a majority of axons in the OT do terminate at the LGN, the OT has a branch carrying some other projections to the hypothalamus, pretectal nuclei, and superior colliculus.¹¹² In this review, we focus on the OT studies at the neuroimaging level at which distinctions between the main route and this branch of the OT are not practically discriminable.

Technical considerations

In general, tracking in the optic chiasm is a difficult task for tractography algorithms, due to the presence of a complex crossing fiber configuration.¹¹³ For this reason, it is common to separately track and identify the ON and OT, to avoid generating erroneous streamlines directly connecting left and right ONs. Tracking the OT in the anterior portion is relatively straightforward since fibers are straight and do not cross with other tracts. However, when the OT gets closer to the LGN, it crosses with various other fiber tracts projecting to other thalamic nuclei and curves into the LGN.

A widely adapted approach to perform the OT tractography is to place ROIs in the optic chiasm and LGN and use these ROIs as a seed for tracking for identifying the OT. While automated identification of the optic chiasm from a T1-weighted image can be easily achieved with the FreeSurfer software,¹¹⁴ the identification of the LGN at the individual level is not very easy since it is not visible in T1-weighted MRI data in a standard resolution. One often needs high-resolution proton-density weighted data to visualize this structure,^{115,116} which is not always practical due to scan time limitations. There are several alternative ways to define the LGN ROI for OT tractography. One strategy is to

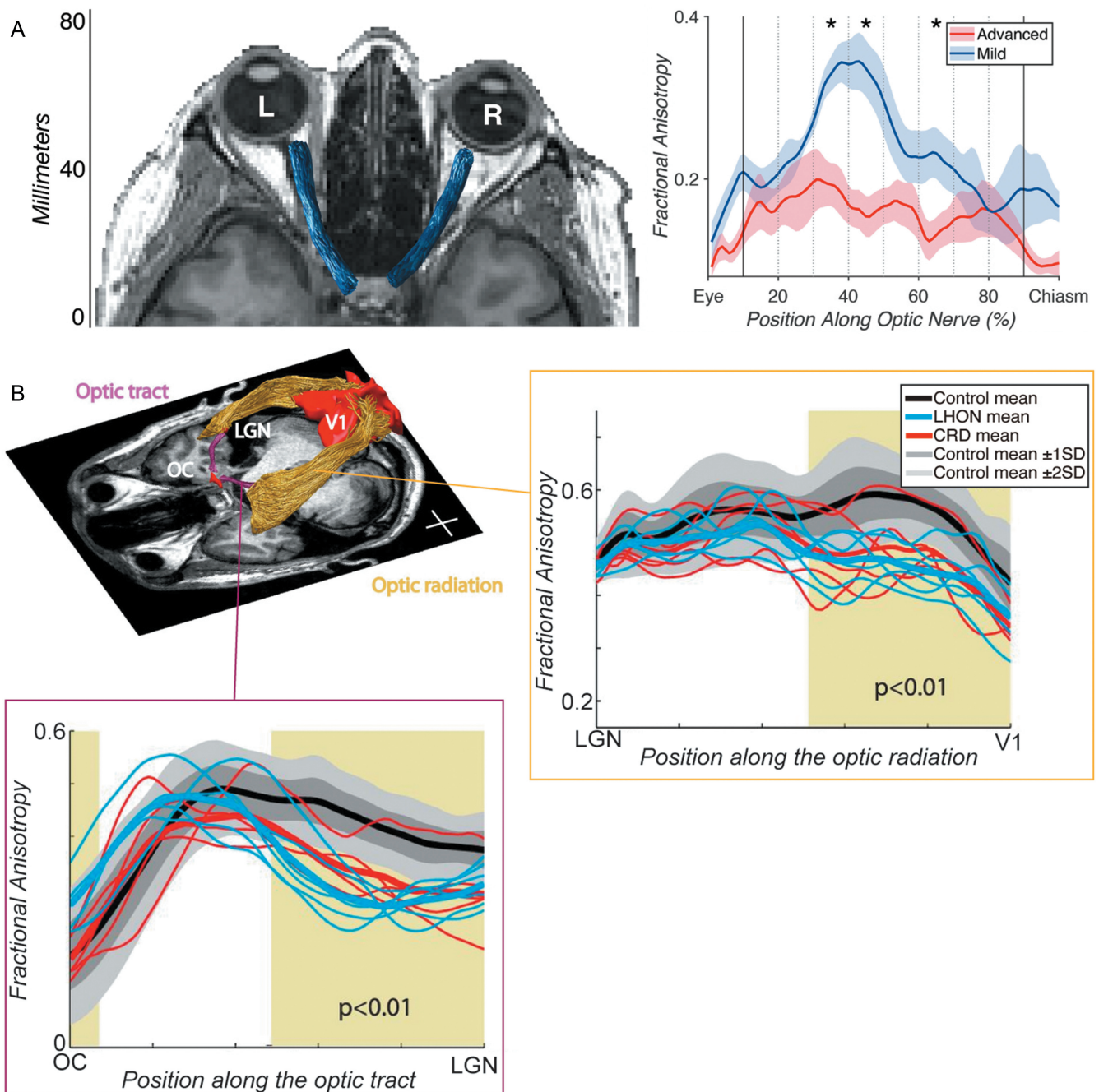


Fig. 4 Tractometry on early visual white matter tracts. **A:** Tractometry study by Miller et al. (2019)¹⁰⁸ focusing on the ON in patients with unilateral advanced-stage glaucoma. *Left panel:* The ON (blue) identified by tractography overlaid on the axial image of structural MRI data. *Right panel:* Tract profiles on dMRI data acquired from patients with unilateral advanced-stage glaucoma, comparing fractional anisotropy (vertical axis) along the ON between eyes with advanced (red) and mild (blue) glaucoma. The horizontal axis describes normalized positions along the ON. Images are adapted from Miller et al. (2019)¹⁰⁸ under the Attribution 4.0 International Creative Commons license (CC BY 4.0). **B:** Tractometry study by Ogawa et al. (2014)¹¹⁸ focusing on the OT and OR in patients with LHON and CRD. *Left top panel:* Tractography on the OT (purple) and OR (yellow) in a representative participant overlaid on an axial slice of a T1-weighted image. The positions of the OC and primary visual cortex (V1) are also depicted. *Left bottom panel:* Tract profiles of the OT, based on dMRI data acquired from patients with LHON (cyan) and CRD (red), and healthy controls. Dark and light gray shadows depict the range of ± 1 SD and ± 2 SD from the control mean. The horizontal axis describes normalized positions along the OT. *Right top panel:* Tract profile of the OR. Conventions are identical to those used in the OT tract profile. Reprinted by permission from reference 118. CRD, cone-rod dystrophy; dMRI, diffusion-weighted MRI; LHON, Leber's hereditary optic neuropathy; OC, optic chiasm; ON, optic nerve; OT, optic tract; OR, optic radiation; SD, standard deviation.

place the seed in the optic chiasm, perform deterministic tractography, and find the location of voxels where streamlines end in the thalamus to estimate a putative position of the LGN.^{117,118} The LGN ROIs estimated by this method roughly match the position of the LGN in anatomical data.¹¹⁹ Kammen and colleagues (2016)¹²⁰ proposed a conceptually similar, but more sophisticated automated approach to identify the LGN ROI from tractography. Specifically, they perform a tracking from the optic chiasm and primary visual cortex (V1) first and then estimate the LGN ROI based on information about where streamlines from the optic chiasm intersect with the thalamus, as well as shape information relative to other structures.¹²⁰ A second strategy is to perform segmentation of thalamic nuclei in the atlas space and try to incorporate the atlas segmentation¹²¹ into the native space to estimate the position of the LGN (implemented in FreeSurfer; <https://freesurfer.net/fswiki/ThalamicNuclei>). Several studies used this strategy to define the LGN ROI as a seed for tracking.^{122,123} Lastly, there are ongoing efforts to improve the segmentation of thalamic nuclei using only dMRI data. If these methods can successfully segment the LGN, it will be ideal since it will allow LGN location identification in the same space.^{124,125} Nevertheless, once researchers can identify the optic chiasm and LGN as seed voxels, the identification of the OT from dMRI in a standard resolution is achievable and widely tested.^{118,126}

Tractometry studies on this tract

A variety of studies used dMRI-based tractometry to evaluate tissue properties of the OT in disorders damaging RGCs and the ON, such as glaucoma,^{127–131} Leber's hereditary optic neuropathy (LHON)^{118,119} (Fig. 4B), and optic neuritis.¹³² These studies show that dMRI-based tractometry has the sensitivity to identify the OT tissue abnormalities that are caused by these disorders. In addition, other lines of tractometry research also showed that tissue abnormalities in the OT can be seen in macular degeneration^{73,118} and amblyopia.¹³³ This series of studies demonstrated that tractometry is a useful approach to evaluate OT tissue changes caused by disorders, although it is not clear whether the tractometry on the OT has sufficient sensitivity to be useful as a tool for clinical application. Another line of neuroscience research investigated to what degree individual variability in the OT is correlated with retinal¹³⁴ or cortical measurements,¹²⁶ among healthy individuals, providing a better understanding of the source of individual variability in the human visual system.^{135–138}

Optic radiation

Anatomy

The optic radiation (OR) is the pathway connecting the LGN and V1. The OR comprises an anterior segment termed "Meyer's loop," which traverses the white matter within the temporal lobe as it circumvents the inferior horn of the lateral ventricle. It is well-documented that lesions affecting

Meyer's loop give rise to a deficit in the upper visual field, implying that this particular segment of the OR conveys information derived from the inferior aspect of the retina. The posterior part of the OR exhibits a rectilinear and anterior–posterior orientation. In its posterior part, the OR passes through a heavily myelinated part of the white matter (the sagittal stratum^{139,140}). Tracer studies performed in the animal brain demonstrated the existence of feedback axons from the LGN to V1.^{141–143} At present, anatomical knowledge regarding how feedforward and feedback axons are organized in the OR is not well established; therefore, researchers need to keep in mind that the OR in tractography analysis does not distinguish the feedforward and feedback pathways. In addition, anatomical connections between the LGN and the secondary visual area (V2) were also reported in macaque tracer studies.^{144,145} While the presence and anatomical trajectory of this pathway in humans remain unclear, it is feasible to employ tractography to detect the connection between the LGN and V2 as a component of the OR.¹⁴⁶ Finally, it is worth noting that a direct axonal projection from the LGN to the middle temporal visual area (area MT), which is an essential area for motion processing, has been reported in an anatomical study on macaque.¹⁴⁷ It is indeed possible to perform tractography between LGN and human MT+ (which is considered to be homologous to macaque MT), with considerable spatial overlap with the OR.^{148–151}

Technical considerations

The challenges for tractography in the OR result from difficulty in tracking Meyer's loop regions. First, it is difficult to reconstruct a curving pathway, such as Meyer's loop, using classical deterministic tractography approaches.^{44,45} While identifying Meyer's loop using deterministic tractography was not impossible,¹⁵² this led to a motivation for developing probabilistic tractography algorithms, which have better sensitivity for thalamo-cortical pathways.^{30,47,153} Second, since Meyer's loop crosses with other white matter tracts, resolving crossing fibers poses challenges for tractography.¹⁵⁴ The acquisition of high-angular resolution dMRI data, together with advanced voxelwise dMRI signals, has provided better sensitivity for OR tractography.^{155,156}

Several tractography strategies dedicated to OR identification have been proposed. For example, Sherbondy and colleagues (2008)⁴⁷ developed a tractography algorithm (ConTrack), which relied on the key idea of separating streamline generation and streamline evaluation. In brief, ConTrack first generates a large set of streamlines connecting two ROIs (LGN and V1) as a candidate of the OR, using a relatively liberal probabilistic tractography algorithm, with many false positives. In the next step, ConTrack calculates the score for each streamline, based on how much the existence of streamline is supported by the diffusion signal in the voxels along its trajectory, as well as how well the shape of each streamline aligns with a prior on the

white matter tract shape. ConTrack reliably identifies the OR, including Meyer's loop.¹¹⁷ In subsequent work, Chamberland and colleagues (2017)¹⁵⁴ proposed an alternative framework for OR tractography, termed MAGNETIC Tractography. In this method, users place ROIs around the medial, anterior, and lateral tip of Meyer's loop, each of which has a preferential tracking direction based on anatomical knowledge. Once a streamline entered the ROI, its tracking direction was guided by the preferred tracking direction of the ROI. This method successfully reconstructed the OR including Meyer's loop from children's dMRI data. Schurr and colleagues (2018)¹⁵⁷ proposed another idea for OR tractography by combining dMRI with myelin-sensitive quantitative T1 (qT1) mapping.^{158,159} Like ConTrack, they separated the process of streamline generation and evaluation. However, instead of using dMRI signals, they used qT1 data to classify which streamline should be assigned to the OR, based on the fact that the OR is more heavily myelinated than neighboring tracts.¹⁶⁰ Thus, streamlines that belong to the OR must pass through areas with a lower qT1. Using qT1 as prior information to filter OR streamlines, they successfully demonstrated an improvement in OR tractography. Aydogan and colleagues (2021)¹⁶¹ proposed a method named "Parallel Transport Tractography," which utilized curve parametrization and incorporated topographic regularities that must exist in white matter tracts. They demonstrated that they successfully identified OR including Meyer's loop.

While these studies and others have provided substantial improvements in methods to identify the OR from dMRI data, there are still interpretive limitations in tractography analysis of the OR. For example, a recent high-resolution anatomical study in vervet monkey brain¹⁶² demonstrated that axons from pulvinar and LGN enter the same part of white matter, and therefore it is difficult to distinguish the OR and axons from pulvinar at the resolution of dMRI. Improved knowledge of human neuroanatomy will further facilitate discussion on more accurate anatomical interpretation of OR tractography.

Tractometry studies on this tract

Many studies have performed tractometry analyses on the OR, to evaluate the impact of visual disorders (see Fig. 4B for an example). Most studies have provided evidence that tissue properties of the OR are significantly different in glaucoma,^{128–130,163–166} LHON,^{118,119} macular degeneration,^{72,73,118} retinitis pigmentosa,¹⁶⁷ and amblyopia,^{133,150,168} as compared with controls. These studies provided converging evidence showing that the tractometry approach is sensitive to trans-synaptic tissue changes in the OR because of disorders at the retinal level. However, open questions remain as to why, in at least some cases, significant effects are found in different dMRI parameters (axial and radial diffusivity) between OT and OR,¹¹⁸ suggesting that underlying

microstructural change occurring in the OR may not be fully the same as those in the OT. One of the possible explanations is that OT and OR exhibit different stages of tissue damage, as it is likely that tissue changes in the OT occur earlier than those in the OR.^{128,129}

The retinotopic organization of V1 is a fundamental property of the visual system that maps function onto structure.^{169–172} A similar retinotopy is known to exist in the structure of the OR, based on selective visual field loss in damage to parts of the OR.¹⁷³ Several studies used this principle to divide the OR into different components, based on retinotopic representation in the V1, and to test visual field specificities of tissue changes occurring in the OR. For example, recent studies used a retinotopy template.^{174–176} to estimate eccentricity representation in V1 and then classify OR streamlines into foveal, mid-periphery, and far-periphery, based on streamline endpoints near V1.^{72,119} These studies found that tissue changes caused by the LHON and macular degeneration are most prominently observed in the OR terminating near foveal V1, consistent with a prediction from the spatial pattern of visual field loss caused by these disorders. Kruper and colleagues (2023)¹⁷⁷ used the same approach to analyze the OR in the data from a large number of healthy participants in the UK Biobank and identified that age dependency in white matter is different among different subcomponents of the OR divided by eccentricity representation in the V1. While these studies suggest that one can separately analyze the OR to evaluate specificity in the visual field, it is not fully clear the extent to which this type of analysis can measure information from axons carrying signals of a specific visual field. Since a study performed in the cat brain suggests that medially and laterally located axons in the OR exchange position along the tract,¹⁷⁸ it is possible that each streamline may not fully reflect axons carrying signals in specific visual fields, posing a general challenge for distinguishing streamlines within the same white matter tract solely based on their endpoints. To improve confidence in these types of analyses, it is essential to further investigate OR neuroanatomy in more detail, which will give us more accurate insights into retinotopic representations of the OR.

In addition to studies focusing on disorders, the tractometry approach on the OR has also been used for various neuroscientific studies. One notable example is a correlation between tissue properties of the visual white matter tracts, such as the OR, and latency of visually evoked potential measured by electroencephalography, in multiple sclerosis patients.^{179,180} Using magnetoencephalography, later studies assessed how individual variability of latency in visually evoked response among healthy adults¹⁸¹ and children¹⁸² is correlated with diffusivity measurements on the OR. Another line of studies also assessed the correlation between OR tissue properties and behavioral and functional measurements related to visual functions, such as eye dominance¹⁸³ and oscillations.^{184,185} Webb and colleagues (2022)¹⁸⁶ reported that age-related differences in tissue properties of

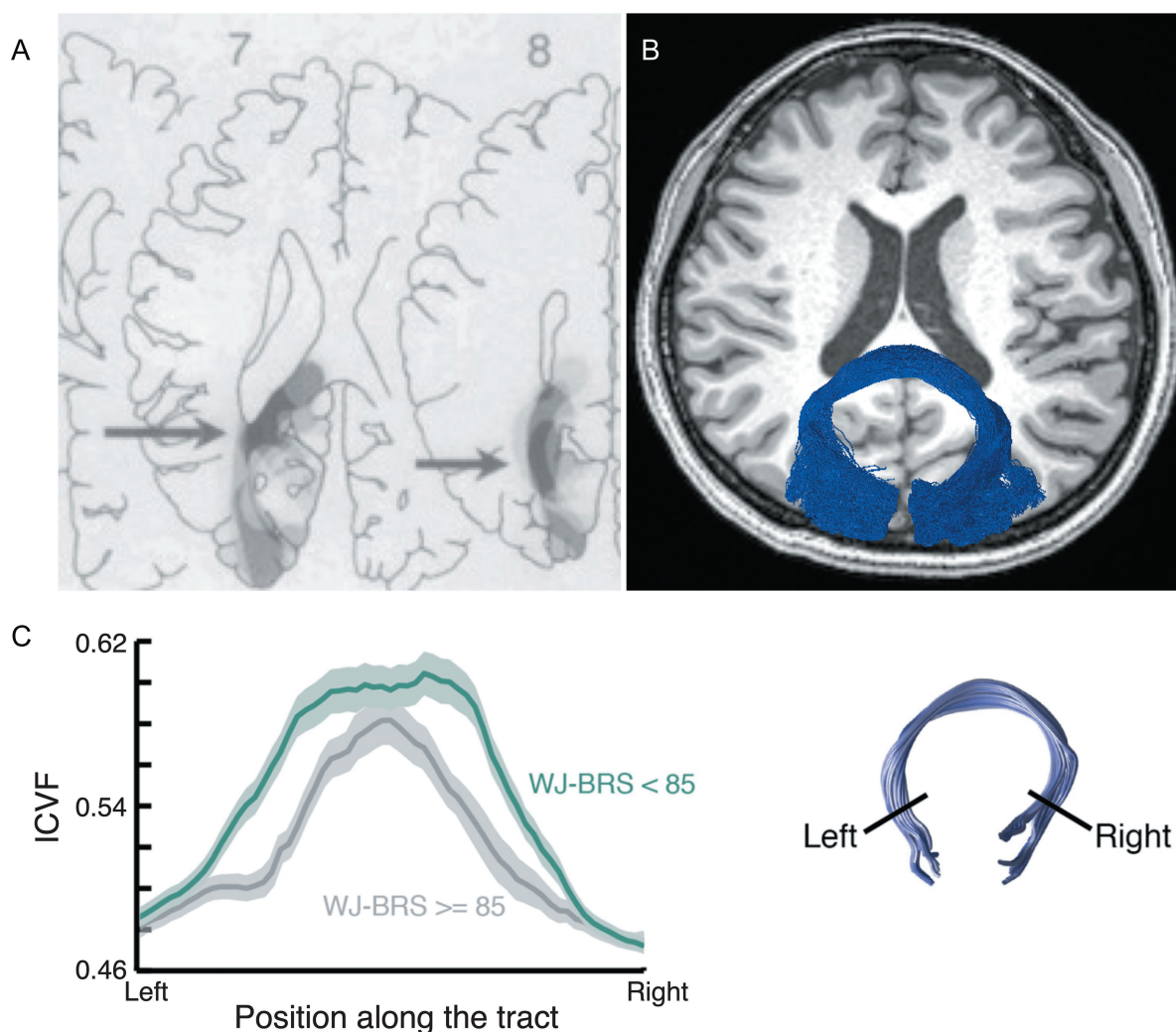


Fig. 5 Forceps major. **A:** The lesion topography of alexia patients.¹⁹¹ The dark gray area (highlighted by arrow) indicates the brain lesion site commonly appeared in alexia patients. This area corresponds to the forceps major. Reprinted by permission from reference 191. **B:** The forceps major (blue) identified by using tractography in dMRI data overlaid on the axial section of a T1-weighted image. **C:** Tractometry study on the forceps major. *Left panel:* Tract profile of the forceps major in good (dark green) and poor readers (gray).²⁰² The horizontal axis depicts the normalized position along the forceps major, whereas the vertical axis depicts microstructural measurement (ICVF estimated by NODDI).³⁴ The shaded area indicates ± 1 s.e.m. The reading performance was measured by the WJ-BRS. *Right panel:* The forceps major identified by tractography. Reprinted by permission from reference 202 (under the CC BY-NC-ND license). dMRI, diffusion-weighted MRI; ICVF, intra-cellular volume fraction; NODDI, neurite orientation dispersion and density imaging; WJ-BRS, Woodcock-Johnson Basic Reading Score.

the OR can predict visual performance, suggesting that the tractometry approach is also useful in considering how aging on the white matter is related to visual functions.

Forceps major

Anatomy

The forceps major is a white matter pathway connecting the bilateral visual cortex and passes through the posterior part of the corpus callosum (Fig. 5B). The callosal portion of this pathway is termed splenium. In anatomical studies, this pathway is also termed “tapetum,” which is a continuum of

fiber pathways from the splenium, and is highly visible in the coronal section of anatomical images. To our knowledge, the precise pattern of anatomical projection of the forceps major is not fully established in humans. While a lesion study investigated this by anatomically examining brains with unilateral occipital infarctions and measuring degenerated axons in the intact hemisphere using silver-staining,¹⁸⁷ most knowledge about this pathway is derived from investigations of apparently homologous pathways in macaque monkey brains. In anatomical studies performed in macaques and humans, it is widely accepted that the

forceps major does not have a projection in the middle portion of the V1, representing the horizontal visual field.^{187–189} Specifically, these studies reported that callosal projection in the human and macaque V1 is restricted near the border between V1 and V2, which represents the vertical meridian of the visual field. The functional significance of this anatomical connection is likely because of the need to integrate information in the left and right visual field, since at the level of V1, the representation of the visual field is predominantly contralateral and this anatomical pathway is needed to process visual information beyond the vertical meridian. This is also in line with a finding in lesion studies demonstrating that pure alexia patients consistently exhibited lesions in the forceps major (Fig. 5A); a lack of this pathway causes reading difficulty at least partly because the integration of left and right visual field becomes difficult.^{190,191} Beyond the V1/V2 border, a precise understanding of the cortical projections of the forceps major in human brains is still a topic of active investigation, using both dMRI and anatomical measurements.¹⁹²

Technical considerations

Identifying the forceps major using tractography is not particularly difficult; for example, one can identify this pathway by simply placing two coronal ROIs in each hemisphere's occipital cortex and selecting streamlines passing through both of them.^{193,194} This protocol is implemented in software for automated tract identification.⁵⁷ The other strategy is to define the splenium as the first sagittal ROI and the entire coronal section posterior to the splenium as the second ROI and then select streamlines passing through both of them as the forceps major.¹⁹⁵ However, the forceps major identified by tractography is often predominantly biased to the bilateral connection between the dorsomedial part of the occipital cortex, as demonstrated by Dougherty et al.¹⁹³ This is most likely because the crossing between the forceps major and OR is difficult to resolve, and therefore identifying the callosal pathway from the ventral part of the occipital cortex is more challenging. Therefore, it is important to keep in mind that tractography reconstruction of the forceps major underrepresents the pathways from the ventral occipito-temporal cortex, due to a sensitivity limit of dMRI.

Tractometry studies on this tract

Initial findings showing that the shape of the corpus callosum in dyslexia patients differs from that in controls existed well before dMRI was invented,^{196,197} but these studies did not focus on splenium and forceps major. Inspired by Binder and Mohr's work,¹⁹¹ which used detailed lesion-symptom mapping to delineate the anatomical basis of reading difficulties in infarct patients, the forceps major is often a target for studies assessing the impact of white matter properties on reading disorders, such as dyslexia.¹⁹⁸

Dougherty and colleagues (2007)¹⁹⁹ segmented the corpus callosum using tractography; they parcellated the corpus callosum based on the origin of streamlines. They observed that diffusivity in the segment of the corpus callosum that receives streamlines from the temporal cortex correlated with phonological awareness in children. The correlation between reading ability and diffusivity in the forceps major (splenium) was also reported in later publications from multiple different laboratories (see Fig. 5C for an example).^{200–202}

Another line of research investigated the relationship between this tract with behavioral or electrophysiological measurements in healthy individuals. For example, Genç and colleagues (2011)²⁰³ performed psychophysical experiments on bistable perception of apparent motion, to quantify how much apparent motion beyond the horizontal meridian is preferentially reported than that beyond the vertical meridian. They found a correlation between these behavioral measurements and diffusivity measurements on the splenium. Another line of research quantified tissue properties of the forceps major and investigated how they relate to electrophysiological measurements on conduction delays between hemispheres.^{204,205} Finally, we note that the presence of abnormality in diffusivity measurements along the forceps major of glaucoma patients has also been reported, suggesting that the impact of glaucoma may not be restricted to primary visual pathways.²⁰⁶

VOF

Anatomy

The VOF is a white matter tract connecting the dorsal and ventral visual cortex, which runs through the lateral side of occipital white matter. It is located lateral to the OR and posterior to the arcuate fasciculus (Fig. 6A).²⁰⁷ Although the existence of this pathway was already known in classical anatomical works performed in the late 19th century, it was neglected until recent dissection (Fig. 6B) and dMRI studies.^{160,208–211} The analysis of the VOF demonstrates that it connects dorsal (V3A/B) and ventral (hV4) parts of the extrastriate cortex,^{207,211,212} suggesting that it has a role in communicating between the dorsal and ventral visual streams, which are involved with spatial and categorical processing, respectively.^{213,214} Another potential role of the VOF is to exchange upper and lower visual field information between dorsal and ventral extrastriate cortex; this type of communication is necessary since V2 and V3 have a split quarterfield representation in dorsal and ventral, but areas anterior to V3 (V3A/B and hV4) represent the entire hemifield.²⁰⁷

The functional significance of the VOF is not fully understood. The pathway may play an important role in reading: Greenblatt (1973)²¹⁵ reported a pure alexia patient with white matter damage in the posterior part of the brain and discussed the relationship with the VOF. This may relate to the fact that the VOF has endpoints near the visual word form

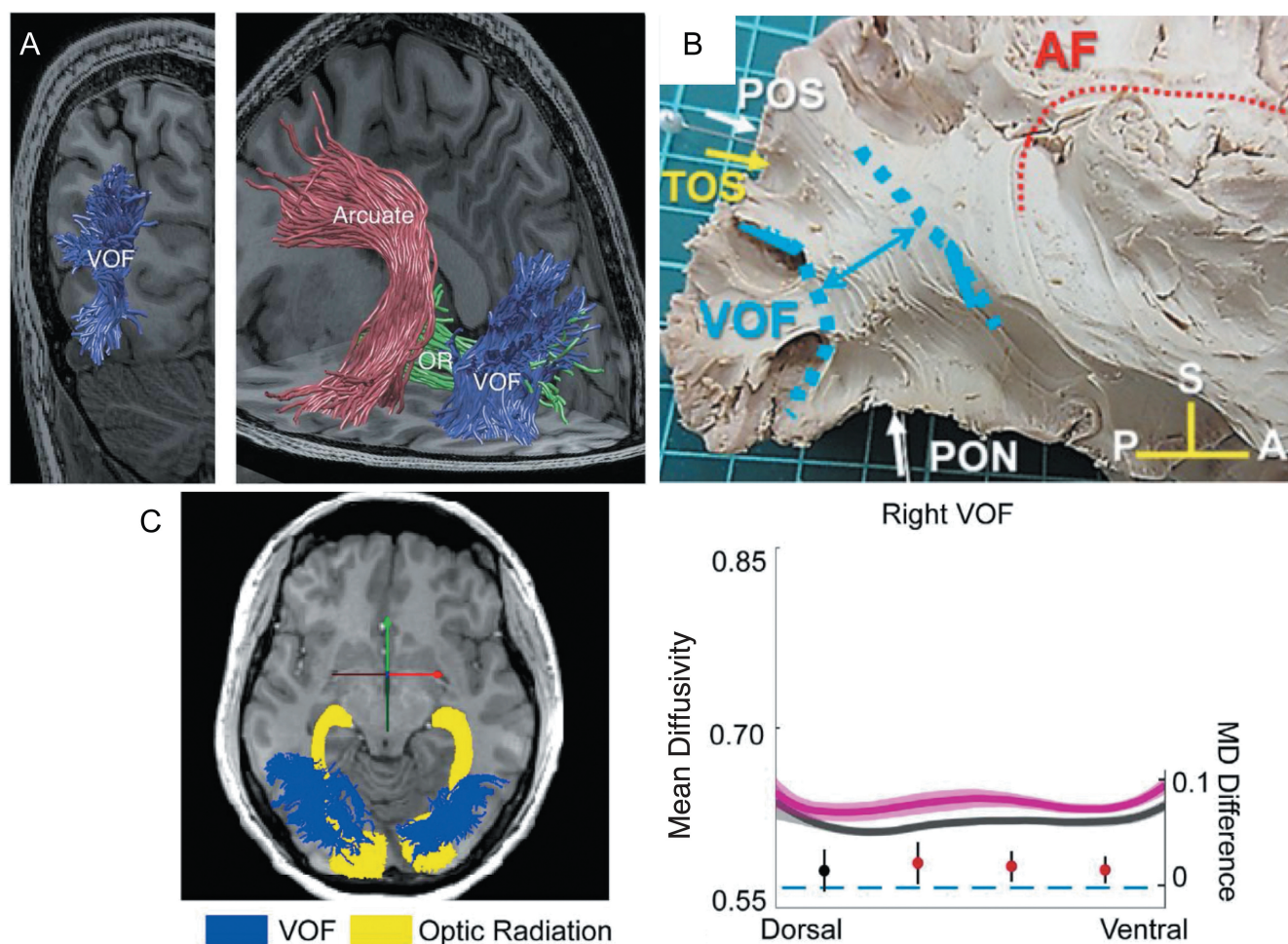


Fig. 6 Vertical occipital fasciculus. **A:** The VOF (blue) is identified by tractography, which is overlaid on a T1-weighted image (left image, coronal view; right image, and sagittal view).²⁰⁷ The VOF is lateral to the OR (green) while posterior to the arcuate fasciculus (red). Reprinted with permission from reference 207. **B:** The VOF identified by Klingler's dissection (highlighted by blue), which is displayed together with other anatomical landmarks.²¹¹ Reprinted by permission from reference 211 (under the Attribution 4.0 International Creative Commons license (CC BY 4.0)). **C:** Tractometry on the VOF on amblyopia patients.¹⁶⁸ *Left panel:* tractometry on the OR (yellow) and VOF (blue) overlaid on a sagittal slice of a T1-weighted image. *Right panel:* tractometry on the right VOF. The amblyopia group (magenta curve) exhibited higher mean diffusivity (vertical axis, unit: $\mu\text{m}^2/\text{s}$) compared with control (dark gray curve). The horizontal axis represents the normalized position along the VOF (left: dorsal, right: ventral). The shadowed area indicates ± 1 s.e.m. from the mean in each group. The filled circles showed differences in mean diffusivity (MD) between amblyopia and the control group (the unit is shown on the right side of the plot). The error bar indicates the 95% confidence interval of the differences. Statistically significant differences were marked in red. Reprinted by permission from reference 168. A, anterior; AF, arcuate fasciculus; OR, optical radiation; P, posterior; PON, pre-occipital notch; POS, parieto-occipital sulcus; S, superior; TOS, transverse occipital sulcus; VOF, vertical occipital fasciculus.

area.²⁰⁸ However, since the lesion described by Greenblatt was not specific to the VOF, it is difficult to conclude the role of the VOF in reading solely based on a case study; this motivates tractometry studies to investigate the relationship between the VOF and reading ability, as discussed below. Another line of work, combining functional MRI (fMRI) and dMRI, suggests a potential role for the VOF in task-dependent activity modulation of the ventral occipito-temporal cortex, which may originate from the dorsal part of the occipital and parietal cortex.²¹⁶

Technical considerations

In general, tensor-based deterministic tractography does not have sufficient sensitivity to delineate this pathway. In our experience, probabilistic tractography with voxelwise diffusion models that have better sensitivity to detect multiple fiber orientations in the voxel, such as constrained spherical deconvolution (CSD; Fig. 1G), is more sensitive to this tract.¹⁶⁰

There are several ROI-based approaches to identify the VOF. One approach is to identify the VOF using ROI based

on gray matter parcellation in the dorsal and ventral occipital cortex; streamlines terminating near both ROIs are identified as the VOF.¹⁶⁰ The second approach is to place two axial waypoint ROIs (one relatively dorsal and the other relatively ventral) in the lateral part of the occipital white matter and to select streamlines passing through both of these ROIs as the VOF.²⁰⁷ In addition to the ROI-based approach, one can include additional constraints for selecting streamlines within the occipital cortex that have the expected vertical orientation.¹⁶⁰ Furthermore, like the approach taken in the OR tractography discussed above, Schurr and colleagues²¹⁷ proposed to use qT1 measurements to identify the VOF, using the fact that the VOF has a lower qT1 from posterior arcuate, which is the tract anterior to the VOF.

Tractometry studies on this tract

Since the VOF has been largely neglected historically,¹⁶⁰ the number of tractometry studies focusing on the VOF remains limited (see Fig. 6C for an example). One notable observation is that some tractometry studies, focusing on amblyopia (Fig. 6C)¹⁶⁸ and binocular stereopsis,²¹⁸ reported group differences in the right VOF only. While some possible functional lateralization in cortical areas connected by the VOF has been reported,²¹⁹ it is uncertain whether these findings reflect functionally meaningful lateralization or possible inter-hemispheric differences in the sensitivity of measurements in this tract. More recent studies performed tractometry analysis on the VOF of multiple sclerosis patients and suggested that differences in diffusivity may explain behavioral deficits.²²⁰

DMRI has also been used to evaluate the relationship between the VOF and reading. Broce and colleagues (2019)²²¹ performed a dMRI study on children and identified that the VOF is involved with early literacy skills of phonological awareness and decoding. The link between the VOF and reading was also identified in a meta-analysis study on stroke,²²² a study predicting reading-related fMRI signal in the ventral occipito-temporal cortex from dMRI data,²²³ and a study investigating the relationship between the hierarchical functional organization of the ventral occipito-temporal cortex and white matter tracts.²²⁴

Future Perspectives and Open Questions

The findings that we have reviewed here demonstrate the utility of tractometry for understanding structure–function relationships in the human visual system from non-invasive dMRI measurements conducted *in vivo*. Tractometry benefits from an approach that capitalizes on the strengths of dMRI measurements, together with anatomical and biophysical knowledge gained from a confluence of many different measurement methods, including invasive and *post-mortem* neuroanatomical techniques.^{225–230} Because of the opportunity to conduct *in vivo* measurements, the methods

and findings of tractometry can translate into important insights into the biological manifestations of individual differences and clinical conditions. Across several different brain connections and in a range of different clinical conditions that we have reviewed, the research consistently shows that differences in visual function correlate with differences in the visual white matter. In some cases, the differences measured in the white matter can be understood as a direct consequence of the disease. For example, diseases that affect the RGCs result in measurable tissue property differences in the ON between patients and matched controls. In addition, in many cases, the research demonstrates a consistent relationship between diseases that affect the retina (e.g., glaucoma, age-related macular degeneration, etc.) and the properties of the white matter further downstream in visual processing. For example, differences between patients and controls in the tissue properties within the ORs are not directly connected to the retina. These changes could arise from trans-synaptic degenerative processes, from activity-dependent plasticity in response to changes to the visual information that is transmitted to the central nervous system, from systemic factors (e.g., small vessel disease in aging, which may affect both the retina and the white matter), or from some combination of these factors. It is worth mentioning that the specific biological processes of regeneration and degeneration of damaged axons are still active targets of research²³¹; therefore, we expect to have more biological information in the future for understanding white matter abnormalities caused by retinal diseases. Disentangling the causal paths and elucidating the biophysics of the differences measured in the white matter remains an important goal for future studies.

How might such progress be made? Tractometry, like many other measurement tools, is limited by the scale of the measurement, by its fidelity, and by its SNR. DMRI is particularly susceptible to a host of interpretive ambiguities. For example, the differences between different groups in terms of the FA of a white matter tract profile can not only arise due to demyelination in one group²³² but also due to differences in the configuration of white matter tissue.⁵⁴ This means that care needs to be taken in interpreting any particular result, and consideration needs to be given to alternative interpretations. Constraining the interpretation of the signal through combinations of different tissue properties and a range of different models can provide an important control on interpretations in terms of specific biological mechanisms. Models that have high test–retest reliability and high accuracy in representing the signal and its biological causes provide a particularly promising path forward in overcoming interpretation limitations of the measurement.^{27,202,233}

Another challenge of dMRI is that the measurements are not strictly quantitative. That is, even though some quantities that are assessed in dMRI data (e.g., mean diffusivity) carry physical units, experiments conducted on different

measurement instruments are affected by the characteristics of the instrument. This means that quantities such as MD and FA may differ within the same subject in measurements conducted on different MRI scanners.^{234,235} Although these effects are not very large, they can be highly consistent, and care needs to be taken to account for these effects, particularly in studies where differences between groups are assessed in unbalanced cohorts measured on different scanners. This challenge is not unique to dMRI data and affects other MRI quantities such as cortical thickness assessed from T1-weighted and T2-weighted imaging,²³⁶ as well as statistics derived from fMRI measurements.^{237,238} Significant research effort has been invested in developing methods for signal harmonization across different scanners^{239–241} but the state of the art in these methods still requires measurements from many different subjects in each scanner.^{242,243} This makes the clinical application of dMRI tractometry challenging because comparing an individual's brain against a normative sample would have to happen either on the same scanner as the one on which the normative sample was acquired or on a scanner that has been harmonized with the scanner used for normative measurements (there are some important exceptions to this rule; for example, where a disease affects lateralization of the measurement²⁴⁴).

For both issues, a particular hope for improvement of the interpretation and clinical utility of tract tissue properties comes from the combination of dMRI tractography with measurements of quantitative MRI (e.g., measurements of qTI mentioned in section “Tractometry of early visual white matter tracts”) within the same individual.^{158,245,246} These methods are relatively more biologically interpretable than the metrics usually derived from dMRI and are less susceptible to differences between MRI scanners. The integration of different MRI measurements will continue to benefit from the consistent improvement in MRI measurements overall, including higher resolution and improved SNR in measurements of dMRI that will help overcome some of the specific challenges that we identified throughout this review.

As mentioned in our review, measurements in clinical populations do indicate consistent differences between groups. What else can be done to improve their clinical utility? In addition to grounding the measurements in biological interpretability and improvements in measurement methods and their integration, another potential direction for future research is to improve the discriminative ability of tractometry. One avenue for such improvements is afforded by harnessing new statistical and machine learning methods with high discriminative accuracy for individual-level prediction.^{247–249} One challenge of developing accurate machine learning models is that their development often requires very large samples.²⁴⁹ Fortunately, measurements of very large samples across the human life span are increasingly available through projects such as the Human Connectome Project,^{250,251} the Healthy Brain Network,^{252,253} the Adolescent Brain Cognitive Development Study,²⁵⁴ the UK Biobank,²⁵⁵ the developing

Human Connectome Project,²⁵⁶ and the Brain/MINDS beyond human brain MRI project.²⁵⁷ By collecting data from populations with a variety of different ages, diseases, and other characteristics, these samples provide excellent opportunities for data-driven discovery using automated tractometry methods and machine learning. However, despite recent claims that some kinds of data analysis require thousands of subjects to provide reproducible inferences,²⁵⁸ we note that reliable and reproducible results may also be obtained even in much smaller samples. This is demonstrated in many of the studies reviewed above when measurements and analysis focus on biological constructs such as tissue properties within brain pathways defined based on the anatomy of every individual, or with detailed measurements within individuals.²⁵⁹ In addition, studies with a smaller number of subjects have advantages^{260,261}: researchers can easily perform repetitive measurements from the same subjects to ensure reproducibility within subjects, utilize clinical records from the same clinician and hospital, obtain extensive multimodal data from the same subjects more easily, carefully visually inspect the data acquired from each subject, and importantly, maximize the flexibility of study designs that allow considering research question in depth. Therefore, we emphasize that large-scale project studies and small-scale laboratory-based studies have complementary roles in advancing our understanding of white matter. From this perspective, the relatively small dataset for rare diseases²⁶² can be just as important as the large public dataset.

In discussing these issues, some consideration needs to be given to the complexities of statistical analysis of tractometry data. In general, tractometry is a very effective approach to mitigating the complexities of statistical analysis, since it substantially reduces the dimensionality of the dataset, while preserving anatomically meaningful structures, which allows researchers to interpret the data in relation to underlying neuroanatomy. However, tract profiles contain a high degree of autocorrelation. That is, neighboring points in a tract profile can hardly be considered independent. This leads to some complexity in considering challenges due to multiple hypothesis tests within a dataset. The simplest and widely taken approach is to average measurements in all points and obtain a single-number summary per tract, to avoid multiplicity in statistical comparisons. However, this approach may potentially miss effects robustly observed in a specific portion of the tract; since axons from different cortical areas can turn into the tract at different positions,²⁶³ it is reasonable to assume that some robust effects can be observed only in a specific portion of the tract. For this reason, tractometry analyses inherently pose a tradeoff between reducing multiplicity and ensuring sensitivity for true effects localized at a specific portion of the tract.

One newly proposed solution to this challenge is to model the full shape of the tract profile using generalized additive models²⁶⁴ (for a recent application of this approach in measurements from the optic radiation see¹⁸⁵). Other similar

approaches use linear mixed effects models where each streamline is considered as a within-subject random factor⁶⁷ or use correction approaches analogous to those used in fMRI.²⁶⁵ One of the benefits of tractometry is that it transforms the hard-to-understand measurements of volumetric MRI data to a tabular “tidy” format,²⁶⁶ while substantially reducing its dimensionality and retaining important information about the biological properties of the measurements. This format is relatively easy to share with and communicate to researchers in data analysis fields, such as statistics and machine learning, and can provide a basis for reproducible and robust inter-disciplinary research.²⁶⁷ The development of reproducible analysis methods using crowd computing, browser-based virtual computing environments, or containerization will further enhance the robustness of tractometry research.^{123,268–270} As part of this effort, we have publicly shared the codes for reproducing the figures in this paper (https://github.com/36000/MRMS_tractometry_review).

While some advances will arise from the development of new measurement techniques and analysis methods, other advances will come from the continued evolution of our understanding of the anatomy and physiology of the white matter. Here, refined definitions and improved taxonomies of the white matter pathways⁸⁴ will provide increased confidence in the interpretation of MRI data. In addition, integrating dMRI with fMRI-based localization and delineation of functional specialization in cortical areas^{208,216,271} and comparative analysis with measurements from other species^{272–274} will provide information about the definition of white matter connections and their functional significance.

Finally, we emphasize that the utility of tractometry depends on the research question. Tractometry is not the right approach if the research question does not align with the spatial scale dMRI offers. Considering the benefits and limitations discussed above, tractometry projects must be designed together with research questions with an appropriate coarseness, in terms of both spatial scales and ambiguity in underlying biological mechanisms. However, as we reviewed in this article, we found that many important questions regarding health and disease can be addressed effectively with tractometry.

Acknowledgments

HT was supported by the Japan Society for the Promotion of Science (JSPS) KAKENHI (JP21H03789 and JP24K03240). AR and JAK were supported through NIH grants MH121868 and EB027585, as well as through NSF grant 1934292. JAK was additionally supported through the NSF Graduate Research Fellowship Program (DGE-2140004).

Conflicts of Interest

Authors declare that no conflict of interest exists regarding this article.

References

- Ramrattan RS, Wolfs RC, Panda-Jonas S, et al. Prevalence and causes of visual field loss in the elderly and associations with impairment in daily functioning: The Rotterdam Study. *Arch Ophthalmol* 2001; 119:1788–1794.
- Prins D, Hanekamp S, Cornelissen FW. Structural brain MRI studies in eye diseases: Are they clinically relevant? A review of current findings. *Acta Ophthalmol* 2016; 94:113–121.
- Azevedo FAC, Carvalho LRB, Grinberg LT, et al. Equal numbers of neuronal and nonneuronal cells make the human brain an isometrically scaled-up primate brain. *J Comp Neurol* 2009; 513:532–541.
- Salami M, Itami C, Tsumoto T, Kimura F. Change of conduction velocity by regional myelination yields constant latency irrespective of distance between thalamus and cortex. *Proc Natl Acad Sci USA* 2003; 100:6174–6179.
- Yakovlev P, Lecours A. The myelogenetic cycles of regional maturation of the brain. In Minkowski A (ed): Regional development of the brain in early life. Philadelphia, FA Davis Co, 1967, 3–70.
- Yeatman JD, Wandell BA, Mezer AA. Lifespan maturation and degeneration of human brain white matter. *Nat Commun* 2014; 5:4932.
- Wake H, Ortiz FC, Woo DH, Lee PR, Angulo MC, Fields RD. Nonsynaptic junctions on myelinating glia promote preferential myelination of electrically active axons. *Nat Commun* 2015; 6:7844.
- Bacmeister CM, Huang R, Osso LA, et al. Motor learning drives dynamic patterns of intermittent myelination on learning-activated axons. *Nat Neurosci* 2022; 25:1300–1313.
- de Faria O Jr., Pivonkova H, Varga B, Timmler S, Evans KA, Káradóttir RT. Periods of synchronized myelin changes shape brain function and plasticity. *Nat Neurosci* 2021; 24:1508–1521.
- Fields RD. Myelination: an overlooked mechanism of synaptic plasticity? *Neuroscientist* 2005; 11:528–531.
- Mount CW, Monje M. Wrapped to adapt: Experience-dependent myelination. *Neuron* 2017; 95:743–756.
- Pease-Raissi SE, Chan JR. Building a (w)rapport between neurons and oligodendroglia: Reciprocal interactions underlying adaptive myelination. *Neuron* 2021; 109:1258–1273.
- Xin W, Chan JR. Myelin plasticity: Sculpting circuits in learning and memory. *Nat Rev Neurosci* 2020; 21:682–694.
- Sampaio-Baptista C, Khrapitchev AA, Foxley S, et al. Motor skill learning induces changes in white matter microstructure and myelination. *J Neurosci* 2013; 33:19499–19503.
- McKenzie IA, Ohayon D, Li H, et al. Motor skill learning requires active central myelination. *Science* 2014; 346:318–322.
- Sampaio-Baptista C, Johansen-Berg H. White matter plasticity in the adult brain. *Neuron* 2017; 96:1239–1251.
- Fields RD. White matter in learning, cognition and psychiatric disorders. *Trends Neurosci* 2008; 31:361–370.
- Mori S, Zhang J. Principles of diffusion tensor imaging and its applications to basic neuroscience research. *Neuron* 2006; 51:527–539.

19. Le Bihan D, Iima M. Diffusion magnetic resonance imaging: What water tells us about biological tissues. *PLoS Biol* 2015; 13:e1002203.
20. Wandell BA. Clarifying human white matter. *Annu Rev Neurosci* 2016; 39:103–128.
21. Rokem A, Takemura H, Bock AS, et al. The visual white matter: The application of diffusion MRI and fiber tractography to vision science. *J Vis* 2017; 17:4.
22. Assaf Y, Johansen-Berg H, Thiebaut de Schotten M. The role of diffusion MRI in neuroscience. *NMR Biomed* 2019; 32:e3762.
23. Stejskal EO, Tanner JE. Spin diffusion measurements: Spin echoes in the presence of a time-dependent field gradient. *J Chem Phys* 1965; 42:288–292.
24. Basser PJ, Mattiello J, LeBihan D. Estimation of the effective self-diffusion tensor from the NMR spin echo. *J Magn Reson B* 1994; 103:247–254.
25. Basser PJ, Pierpaoli C. Microstructural and physiological features of tissues elucidated by quantitative-diffusion-tensor MRI. *J Magn Reson B* 1996; 111:209–219.
26. Pierpaoli C, Basser PJ. Toward a quantitative assessment of diffusion anisotropy. *Magn Reson Med* 1996; 36:893–906.
27. Rokem A, Yeatman JD, Pestilli F, et al. Evaluating the accuracy of diffusion MRI models in white matter. *PLoS One* 2015; 10:e0123272.
28. Kruper J, Yeatman JD, Richie-Halford A, et al. Evaluating the reliability of human brain white matter tractometry. *Apert Neuro* 2021; 1:1–25.
29. Frank LR. Anisotropy in high angular resolution diffusion-weighted MRI. *Magn Reson Med* 2001; 45:935–939.
30. Behrens TEJ, Woolrich MW, Jenkinson M, et al. Characterization and propagation of uncertainty in diffusion-weighted MR imaging. *Magn Reson Med* 2003; 50:1077–1088.
31. Tournier JD, Calamante F, Connelly A. Robust determination of the fibre orientation distribution in diffusion MRI: Non-negativity constrained super-resolved spherical deconvolution. *Neuroimage* 2007; 35:1459–1472.
32. Assaf Y, Freidlin RZ, Rohde GK, Basser PJ. New modeling and experimental framework to characterize hindered and restricted water diffusion in brain white matter. *Magn Reson Med* 2004; 52:965–978.
33. Assaf Y, Blumenfeld-Katzir T, Yovel Y, Basser PJ. AxCaliber: A method for measuring axon diameter distribution from diffusion MRI. *Magn Reson Med* 2008; 59:1347–1354.
34. Zhang H, Schneider T, Wheeler-Kingshott CA, Alexander DC. NODDI: Practical in vivo neurite orientation dispersion and density imaging of the human brain. *Neuroimage* 2012; 61:1000–1016.
35. Kaden E, Kelm ND, Carson RP, Does MD, Alexander DC. Multi-compartment microscopic diffusion imaging. *Neuroimage* 2016; 139:346–359.
36. Palombo M, Ianus A, Guerreri M, et al. SANDI: A compartment-based model for non-invasive apparent soma and neurite imaging by diffusion MRI. *Neuroimage* 2020; 215:116835.
37. Parker GD, Marshall D, Rosin PL, Drage N, Richmond S, Jones DK. A pitfall in the reconstruction of fibre ODFs using spherical deconvolution of diffusion MRI data. *Neuroimage* 2013; 65:433–448.
38. Jelescu IO, Veraart J, Fieremans E, Novikov DS. Degeneracy in model parameter estimation for multi-compartmental diffusion in neuronal tissue. *NMR Biomed* 2016; 29:33–47.
39. Jeurissen B, Leemans A, Tournier J-D, Jones DK, Sijbers J. Investigating the prevalence of complex fiber configurations in white matter tissue with diffusion magnetic resonance imaging. *Hum Brain Mapp* 2013; 34:2747–2766.
40. Dell'Acqua F, Rizzo G, Scifo P, Clarke RA, Scotti G, Fazio F. A model-based deconvolution approach to solve fiber crossing in diffusion-weighted MR imaging. *IEEE Trans Biomed Eng* 2007; 54: 462–472.
41. Behrens TE, Berg HJ, Jbabdi S, Rushworth MF, Woolrich MW. Probabilistic diffusion tractography with multiple fiber orientations: What can we gain? *Neuroimage* 2007; 34:144–155.
42. Tournier J-D, Yeh C-H, Calamante F, Cho K-H, Connelly A, Lin C-P. Resolving crossing fibres using constrained spherical deconvolution: Validation using diffusion-weighted imaging phantom data. *Neuroimage* 2008; 42:617–625.
43. Basser PJ, Pajevic S, Pierpaoli C, Duda J, Aldroubi A. In vivo fiber tractography using DT-MRI data. *Magn Reson Med* 2000; 44:625–632.
44. Mori S, Crain BJ, Chacko VP, van Zijl PC. Three-dimensional tracking of axonal projections in the brain by magnetic resonance imaging. *Ann Neurol* 1999; 45:265–269.
45. Conturo TE, Lori NF, Cull TS, et al. Tracking neuronal fiber pathways in the living human brain. *Proc Natl Acad Sci USA* 1999; 96:10422–10427.
46. Parker GJM, Haroon HA, Wheeler-Kingshott CAM. A framework for a streamline-based probabilistic index of connectivity (PICO) using a structural interpretation of MRI diffusion measurements. *J Magn Reson Imaging* 2003; 18:242–254.
47. Sherbondy AJ, Dougherty RF, Ben-Shachar M, Napel S, Wandell BA. ConTrack: Finding the most likely pathways between brain regions using diffusion tractography. *J Vis* 2008; 8:15.1–16.
48. Smith RE, Tournier JD, Calamante F, Connelly A. SIFT: Spherical-deconvolution informed filtering of tractograms. *Neuroimage* 2013; 67:298–312.
49. Smith RE, Tournier JD, Calamante F, Connelly A. The effects of SIFT on the reproducibility and biological accuracy of the structural connectome. *Neuroimage* 2015; 104:253–265.
50. Smith RE, Tournier JD, Calamante F, Connelly A. SIFT2: Enabling dense quantitative assessment of brain white matter connectivity using streamlines tractography. *Neuroimage* 2015; 119:338–351.
51. Pestilli F, Yeatman JD, Rokem A, Kay KN, Wandell BA. Evaluation and statistical inference for human connectomes. *Nat Methods* 2014; 11:1058–1063.
52. Daducci A, Dal Palù A, Lemkaddem A, Thiran J-P. COMMIT: Convex optimization modeling for microstructure informed tractography. *IEEE Trans Med Imaging* 2015; 34:246–257.

53. Takemura H, Caiafa CF, Wandell BA, Pestilli F. Ensemble tractography. *PLoS Comput Biol* 2016; 12:e1004692.
54. Jones DK, Knösche TR, Turner R. White matter integrity, fiber count, and other fallacies: The do's and don'ts of diffusion MRI. *Neuroimage* 2013; 73:239–254.
55. Maier-Hein KH, Neher PF, Houde J-C, et al. The challenge of mapping the human connectome based on diffusion tractography. *Nat Commun* 2017; 8:1349.
56. Schilling KG, Petit L, Rheault F, et al. Brain connections derived from diffusion MRI tractography can be highly anatomically accurate-if we know where white matter pathways start, where they end, and where they do not go. *Brain Struct Funct* 2020; 225:2387–2402.
57. Yeatman JD, Dougherty RF, Myall NJ, Wandell BA, Feldman HM. Tract profiles of white matter properties: Automating fiber-tract quantification. *PLoS One* 2012; 7:e49790.
58. Catani M, Howard RJ, Pajevic S, Jones DK. Virtual in vivo interactive dissection of white matter fasciculi in the human brain. *Neuroimage* 2002; 17:77–94.
59. Wakana S, Jiang H, Nagae-Poetscher LM, van Zijl PCM, Mori S. Fiber tract-based atlas of human white matter anatomy. *Radiology* 2004; 230: 77–87.
60. Gerig G, Gouttard S, Corouge I. Analysis of brain white matter via fiber tract modeling. *Conf Proc IEEE Eng Med Biol Soc* 2004; 2004:4421–4424.
61. Jones DK, Travis AR, Eden G, Pierpaoli C, Basser PJ. PASTA: Pointwise assessment of streamline tractography attributes. *Magn Reson Med* 2005; 53:1462–1467.
62. Yendiki A, Panneck P, Srinivasan P, et al. Automated probabilistic reconstruction of white-matter pathways in health and disease using an atlas of the underlying anatomy. *Front Neuroinform* 2011; 5:23.
63. Garyfallidis E, Côté M-A, Rheault F, et al. Recognition of white matter bundles using local and global streamline-based registration and clustering. *Neuroimage* 2018; 170:283–295.
64. Wasserthal J, Neher P, Maier-Hein KH. TractSeg - Fast and accurate white matter tract segmentation. *Neuroimage* 2018; 183: 239–253.
65. Wassermann D, Makris N, Rathi Y, et al. The white matter query language: A novel approach for describing human white matter anatomy. *Brain Struct Funct* 2016; 221:4705–4721.
66. Warrington S, Bryant KL, Khrapitchev AA, et al. XTRACT - Standardised protocols for automated tractography in the human and macaque brain. *Neuroimage* 2020; 217:116923.
67. Chandio BQ, Risacher SL, Pestilli F, et al. Bundle analytics, a computational framework for investigating the shapes and profiles of brain pathways across populations. *Sci Rep* 2020; 10:17149.
68. Andica C, Kamagata K, Aoki S. Automated three-dimensional major white matter bundle segmentation using diffusion magnetic resonance imaging. *Anat Sci Int* 2023; 98:318–336.
69. Kamagata K, Andica C, Uchida W, et al. Advancements in diffusion MRI tractography for neurosurgery. *Invest Radiol* 2024; 59:13–25.
70. Lipp I, Parker GD, Tallantyre EC, et al. Tractography in the presence of multiple sclerosis lesions. *Neuroimage* 2020; 209:116471.
71. Raz N, Levin N. Cortical and white matter mapping in the visual system-more than meets the eye: on the importance of functional imaging to understand visual system pathologies. *Front Integr Neurosci* 2014; 8:68.
72. Yoshimine S, Ogawa S, Horiguchi H, et al. Age-related macular degeneration affects the optic radiation white matter projecting to locations of retinal damage. *Brain Struct Funct* 2018; 223:3889–3900.
73. Malania M, Konrad J, Jäggle H, Werner JS, Greenlee MW. Compromised integrity of central visual pathways in patients with macular degeneration. *Invest Ophthalmol Vis Sci* 2017; 58:2939–2947.
74. Hartong DT, Berson EL, Dryja TP. Retinitis pigmentosa. *Lancet* 2006; 368:1795–1809.
75. Quigley HA, Dunkelberger GR, Green WR. Retinal ganglion cell atrophy correlated with automated perimetry in human eyes with glaucoma. *Am J Ophthalmol* 1989; 107:453–464.
76. Palanker D, Le Mer Y, Mohand-Said S, Sahel JA. Simultaneous perception of prosthetic and natural vision in AMD patients. *Nat Commun* 2022; 13:513.
77. Fujikado T, Kamei M, Sakaguchi H, et al. One-year outcome of 49-channel suprachoroidal-transretinal stimulation prosthesis in patients with advanced retinitis pigmentosa. *Invest Ophthalmol Vis Sci* 2016; 57:6147–6157.
78. Beauchamp MS, Oswald D, Sun P, et al. Dynamic stimulation of visual cortex produces form vision in sighted and blind humans. *Cell* 2020; 181:774–783.e5.
79. Mandai M, Watanabe A, Kurimoto Y, et al. Autologous induced stem-cell-derived retinal cells for macular degeneration. *N Engl J Med* 2017; 376:1038–1046.
80. Gomez J, Pestilli F, Witthoft N, et al. Functionally defined white matter reveals segregated pathways in human ventral temporal cortex associated with category-specific processing. *Neuron* 2015; 85:216–227.
81. Grill-Spector K, Weiner KS, Kay K, Gomez J. The functional neuroanatomy of human face perception. *Annu Rev Vis Sci* 2017; 3:167–196.
82. Catani M, Thiebaut de Schotten M. Atlas of human brain connections. Oxford:Oxford University Press, 2012.
83. Catani M, Thiebaut de Schotten M. A diffusion tensor imaging tractography atlas for virtual in vivo dissections. *Cortex* 2008; 44:1105–1132.
84. Bullock DN, Hayday EA, Grier MD, Tang W, Pestilli F, Heilbronner SR. A taxonomy of the brain's white matter: Twenty-one major tracts for the 21st century. *Cereb Cortex* 2022; 32: 4524–4548.
85. Hanekamp S, Čurčić-Blake B, Caron B, et al. White matter alterations in glaucoma and monocular blindness differ outside the visual system. *Sci Rep* 2021; 11:6866.
86. Forkel SJ, Mahmood S, Vergani F, Catani M. The white matter of the human cerebrum: Part I The occipital lobe by Heinrich Sachs. *Cortex* 2015; 62:182–202.
87. Bugain M, Dimech Y, Torzhenskaya N, et al. Occipital Intralobar fasciculi: A description, through tractography, of three forgotten tracts. *Commun Biol* 2021; 4:433.

88. Andersson JLR, Skare S, Ashburner J. How to correct susceptibility distortions in spin-echo echo-planar images: Application to diffusion tensor imaging. *Neuroimage* 2003; 20:870–888.
89. Carrozzi A, Gramegna LL, Sighinolfi G, et al. Methods of diffusion MRI tractography for localization of the anterior optic pathway: A systematic review of validated methods. *Neuroimage Clin* 2023; 39:103494.
90. He J, Zhang F, Xie G, et al. Comparison of multiple tractography methods for reconstruction of the retinogeniculate visual pathway using diffusion MRI. *Hum Brain Mapp* 2021; 42:3887–3904.
91. Kruper J, Rokem A. Automatic fast and reliable recognition of a small brain white matter bundle. Computational Diffusion MRI: 14th International Workshop, CDMRI 2023, Held in Conjunction with MICCAI 2023, Vancouver, BC, Canada, October 8, 2023, Proceedings, Berlin, Heidelberg, 2024; 70–79.
92. Wheeler-Kingshott CAM, Trip SA, Symms MR, Parker GJM, Barker GJ, Miller DH. In vivo diffusion tensor imaging of the human optic nerve: Pilot study in normal controls. *Magn Reson Med* 2006; 56:446–451.
93. Trip SA, Wheeler-Kingshott C, Jones SJ, et al. Optic nerve diffusion tensor imaging in optic neuritis. *Neuroimage* 2006; 30:498–505.
94. Wheeler-Kingshott CAM, Parker GJM, Symms MR, et al. ADC mapping of the human optic nerve: increased resolution, coverage, and reliability with CSF-suppressed ZOOM-EPI. *Magn Reson Med* 2002; 47:24–31.
95. Hickman SJ, Wheeler-Kingshott CAM, Jones SJ, et al. Optic nerve diffusion measurement from diffusion-weighted imaging in optic neuritis. *AJNR Am J Neuroradiol* 2005; 26:951–956.
96. Kolbe S, Chapman C, Nguyen T, et al. Optic nerve diffusion changes and atrophy jointly predict visual dysfunction after optic neuritis. *Neuroimage* 2009; 45:679–686.
97. Porter DA, Heidemann RM. High resolution diffusion-weighted imaging using readout-segmented echo-planar imaging, parallel imaging and a two-dimensional navigator-based reacquisition. *Magn Reson Med* 2009; 62:468–475.
98. Yeom KW, Holdsworth SJ, Van AT, et al. Comparison of readout-segmented echo-planar imaging (EPI) and single-shot EPI in clinical application of diffusion-weighted imaging of the pediatric brain. *AJR Am J Roentgenol* 2013; 200:W437–443.
99. Wan H, Sha Y, Zhang F, Hong R, Tian G, Fan H. Diffusion-weighted imaging using readout-segmented echo-planar imaging, parallel imaging, and two-dimensional navigator-based reacquisition in detecting acute optic neuritis. *J Magn Reson Imaging* 2016; 43:655–660.
100. Yamada H, Yamamoto A, Okada T, et al. Diffusion tensor imaging of the optic chiasm in patients with intra- or parasellar tumor using readout-segmented echo-planar. *Magn Reson Imaging* 2016; 34:654–661.
101. Seeger A, Schulze M, Schuettauf F, Ernemann U, Hauser T-K. Advanced diffusion-weighted imaging in patients with optic neuritis deficit - value of reduced field of view DWI and readout-segmented DWI. *Neuroradiol J* 2018; 31:126–132.
102. Chen HH, Hu H, Chen W, et al. Thyroid-associated orbitopathy: Evaluating microstructural changes of extraocular muscles and optic nerves using readout-segmented echo-planar imaging-based diffusion tensor imaging. *Korean J Radiol* 2020; 21:332–340.
103. Zhou F, Li Q, Zhang X, et al. Reproducibility and feasibility of optic nerve diffusion MRI techniques: Single-shot echo-planar imaging (EPI), readout-segmented EPI, and reduced field-of-view diffusion-weighted imaging. *BMC Med Imaging* 2022; 22:96.
104. Frost R, Jezzard P, Douaud G, Clare S, Porter DA, Miller KL. Scan time reduction for readout-segmented EPI using simultaneous multislice acceleration: Diffusion-weighted imaging at 3 and 7 Tesla. *Magn Reson Med* 2015; 74:136–149.
105. Takemura H, Liu W, Kuribayashi H, Miyata T, Kida I. Evaluation of simultaneous multi-slice readout-segmented diffusion-weighted MRI acquisition in human optic nerve measurements. *Magn Reson Imaging* 2023; 102:103–114.
106. Estrada S, Kügler D, Bahrami E, et al. FastSurfer-HypVINN: Automated sub-segmentation of the hypothalamus and adjacent structures on high-resolution brain MRI. *Imaging Neurosci* 2023; 1:1–32.
107. Garaci FG, Bolacchi F, Cerulli A, et al. Optic nerve and optic radiation neurodegeneration in patients with glaucoma: In vivo analysis with 3-T diffusion-tensor MR imaging. *Radiology* 2009; 252:496–501.
108. Miller N, Liu Y, Krivochenitser R, Rokers B. Linking neural and clinical measures of glaucoma with diffusion magnetic resonance imaging (dMRI). *PLoS One* 2019; 14:e0217011.
109. Haykal S, Jansonius NM, Cornelissen FW. Investigating changes in axonal density and morphology of glaucomatous optic nerves using fixel-based analysis. *Eur J Radiol* 2020; 133:109356.
110. Hong EH, Yang J-J, Yeon Y, et al. Quantitative evaluation of intraorbital optic nerve in optic atrophy using diffusion tensor imaging. *Sci Rep* 2022; 12:12103.
111. Moon Y, Yang J-J, Lee WJ, Lee JY, Kim YJ, Lim HW. In vivo analysis of normal optic nerve in an elderly population using diffusion magnetic resonance imaging tractography. *Front Neurol* 2021; 12:680488.
112. Mai JK, Paxinos G. The Human Nervous System. third edition. Academic Press, 2011.
113. Roebroek A, Galuske R, Formisano E, et al. High-resolution diffusion tensor imaging and tractography of the human optic chiasm at 9.4 T. *Neuroimage* 2008; 39:157–168.
114. Fischl B. FreeSurfer. *Neuroimage* 2012; 62:774–781.
115. Viviano JD, Schneider KA. Interhemispheric interactions of the human thalamic reticular nucleus. *J Neurosci* 2015; 35:2026–2032.
116. Oishi H, Takemura H, Amano K. Macromolecular tissue volume mapping of lateral geniculate nucleus subdivisions in living human brains. *Neuroimage* 2023; 265:119777.
117. Sherbondy AJ, Dougherty RF, Napel S, Wandell BA. Identifying the human optic radiation using diffusion imaging and fiber tractography. *J Vis* 2008; 8:12.1–11.

118. Ogawa S, Takemura H, Horiguchi H, et al. White matter consequences of retinal receptor and ganglion cell damage. *Invest Ophthalmol Vis Sci* 2014; 55:6976–6986.
119. Takemura H, Ogawa S, Mezer AA, et al. Diffusivity and quantitative T1 profile of human visual white matter tracts after retinal ganglion cell damage. *Neuroimage Clin* 2019; 23:101826.
120. Kammen A, Law M, Tjan BS, Toga AW, Shi Y. Automated retinofugal visual pathway reconstruction with multi-shell HARDI and FOD-based analysis. *Neuroimage* 2016; 125:767–779.
121. Iglesias JE, Insausti R, Lerma-Usabiaga G, et al. A probabilistic atlas of the human thalamic nuclei combining ex vivo MRI and histology. *Neuroimage* 2018; 183:314–326.
122. Liu M, Lerma-Usabiaga G, Clascá F, Paz-Alonso PM. Reproducible protocol to obtain and measure first-order relay human thalamic white-matter tracts. *Neuroimage* 2022; 262:119558.
123. Lerma-Usabiaga G, Liu M, Paz-Alonso PM, Wandell BA. Reproducible Tract Profiles 2 (RTP2) suite, from diffusion MRI acquisition to clinical practice and research. *Sci Rep* 2023; 13:6010.
124. Tregidgo HFJ, Soskic S, Olchanyi MD, et al. Domain-agnostic segmentation of thalamic nuclei from joint structural and diffusion MRI. Medical Image Computing and Computer Assisted Intervention – MICCAI 2023, 2023; 247–257.
125. Tregidgo HFJ, Soskic S, Althonayan J, et al. Accurate Bayesian segmentation of thalamic nuclei using diffusion MRI and an improved histological atlas. *Neuroimage* 2023; 274:120129.
126. Miyata T, Benson NC, Winawer J, Takemura H. Structural covariance and heritability of the optic tract and primary visual cortex in living human brains. *J Neurosci* 2022; 42:6761–6769.
127. Zhou W, Muir ER, Chalfin S, Nagi KS, Duong TQ. MRI study of the posterior visual pathways in primary open angle glaucoma. *J Glaucoma* 2017; 26:173–181.
128. Haykal S, Curcic-Blake B, Jansonius NM, Cornelissen FW. Fixel-based analysis of visual pathway white matter in primary open-angle glaucoma. *Invest Ophthalmol Vis Sci* 2019; 60:3803–3812.
129. Haykal S, Jansonius NM, Cornelissen FW. Progression of visual pathway degeneration in primary open-angle glaucoma: A longitudinal study. *Front Hum Neurosci* 2021; 15:630898.
130. Ogawa S, Takemura H, Horiguchi H, et al. Multi-contrast magnetic resonance imaging of visual white matter pathways in patients with glaucoma. *Invest Ophthalmol Vis Sci* 2022; 63:29.
131. Haykal S, Invernizzi A, Carvalho J, Jansonius NM, Cornelissen FW. Microstructural visual pathway white matter alterations in primary open-angle glaucoma: A neurite orientation dispersion and density imaging study. *AJNR Am J Neuroradiol* 2022; 43:756–763.
132. Backner Y, Kuchling J, Massarwa S, et al. Anatomical wiring and functional networking changes in the visual system following optic neuritis. *JAMA Neurol* 2018; 75:287–295.
133. Allen B, Schmitt MA, Kushner BJ, Rokers B. Retinothalamic white matter abnormalities in amblyopia. *Invest Ophthalmol Vis Sci* 2018; 59:921–929.
134. Taskin HO, Qiao Y, Sydnor VJ, et al. Retinal ganglion cell endowment is correlated with optic tract fiber cross section, not density. *Neuroimage* 2022; 260:119495.
135. Andrews TJ, Halpern SD, Purves D. Correlated size variations in human visual cortex, lateral geniculate nucleus, and optic tract. *J Neurosci* 1997; 17:2859–2868.
136. Dougherty RF, Koch VM, Brewer AA, Fischer B, Modersitzki J, Wandell BA. Visual field representations and locations of visual areas V1/2/3 in human visual cortex. *J Vis* 2003; 3:586–598.
137. Schwarzkopf DS, Song C, Rees G. The surface area of human V1 predicts the subjective experience of object size. *Nat Neurosci* 2011; 14:28–30.
138. Benson NC, Yoon JMD, Forenzo D, Engel SA, Kay KN, Winawer J. Variability of the surface area of the V1, V2, and V3 maps in a large sample of human observers. *J Neurosci* 2022; 42:8629–8646.
139. Di Carlo DT, Benedetto N, Duffau H, et al. Microsurgical anatomy of the sagittal stratum. *Acta Neurochir (Wien)* 2019; 161:2319–2327.
140. Maldonado IL, Destrieux C, Ribas EC, Siqueira de Abreu Brito Guimarães B, Cruz PP, Duffau H. Composition and organization of the sagittal stratum in the human brain: A fiber dissection study. *J Neurosurg* 2021; 135:1214–1222.
141. Ichida JM, Casagrande VA. Organization of the feedback pathway from striate cortex (V1) to the lateral geniculate nucleus (LGN) in the owl monkey (*Aotus trivirgatus*). *J Comp Neurol* 2002; 454:272–283.
142. Angelucci A, Sainsbury K. Contribution of feedforward thalamic afferents and corticogeniculate feedback to the spatial summation area of macaque V1 and LGN. *J Comp Neurol* 2006; 498:330–351.
143. Briggs F, Usrey WM. Corticogeniculate feedback and visual processing in the primate. *J Physiol* 2011; 589:33–40.
144. Yukie M, Iwai E. Direct projection from the dorsal lateral geniculate nucleus to the prestriate cortex in macaque monkeys. *J Comp Neurol* 1981; 201:81–97.
145. Briggs F, Kiley CW, Callaway EM, Usrey WM. Morphological substrates for parallel streams of corticogeniculate feedback originating in both V1 and V2 of the macaque monkey. *Neuron* 2016; 90:388–399.
146. Alvarez I, Schwarzkopf DS, Clark CA. Extrastriate projections in human optic radiation revealed by fMRI-informed tractography. *Brain Struct Funct* 2015; 220:2519–2532.
147. Sincich LC, Park KF, Wohlgenuth MJ, Horton JC. Bypassing V1: A direct geniculate input to area MT. *Nat Neurosci* 2004; 7:1123–1128.
148. Ajina S, Pestilli F, Rokem A, Kennard C, Bridge H. Human blindsight is mediated by an intact geniculo-extrastriate pathway. *eLife* 2015; 4:e08935.
149. Ajina S, Bridge H. Subcortical pathways to extrastriate visual cortex underlie residual vision following bilateral damage to V1. *Neuropsychologia* 2019; 128:140–149.
150. Allen B, Spiegel DP, Thompson B, Pestilli F, Rokers B. Altered white matter in early visual pathways of humans with amblyopia. *Vision Res* 2015; 114:48–55.
151. Pedersini CA, Lingnau A, Cardobi N, Sanchez-Lopez J, Savazzi S, Marzi CA. Neural bases of visual processing of moving and stationary stimuli presented to the blind

- hemifield of hemianopic patients. *Neuropsychologia* 2020; 141:107430.
152. Yamamoto A, Miki Y, Urayama S, et al. Diffusion tensor fiber tractography of the optic radiation: Analysis with 6-, 12-, 40-, and 81-directional motion-probing gradients, a preliminary study. *AJNR Am J Neuroradiol* 2007; 28:92–96.
 153. Behrens TEJ, Johansen-Berg H, Woolrich MW, et al. Non-invasive mapping of connections between human thalamus and cortex using diffusion imaging. *Nat Neurosci* 2003; 6:750–757.
 154. Chamberland M, Scherrer B, Prabhu SP, et al. Active delineation of Meyer's loop using oriented priors through MAGNETic tractography (MAGNET). *Hum Brain Mapp* 2017; 38:509–527.
 155. Tournier JD, Calamante F, Connelly A. MRtrix: Diffusion tractography in crossing fiber regions. *Int J Imaging Syst Technol* 2012; 22:53–66.
 156. Chamberland M, Tax CMW, Jones DK. Meyer's loop tractography for image-guided surgery depends on imaging protocol and hardware. *Neuroimage Clin* 2018; 20:458–465.
 157. Schurr R, Duan Y, Norcia AM, Ogawa S, Yeatman JD, Mezer AA. Tractography optimization using quantitative T1 mapping in the human optic radiation. *Neuroimage* 2018; 181:645–658.
 158. Mezer A, Yeatman JD, Stikov N, et al. Quantifying the local tissue volume and composition in individual brains with magnetic resonance imaging. *Nat Med* 2013; 19:1667–1672.
 159. Stüber C, Morawski M, Schafer A, et al. Myelin and iron concentration in the human brain: A quantitative study of MRI contrast. *Neuroimage* 2014; 93:95–106.
 160. Yeatman JD, Weiner KS, Pestilli F, Rokem A, Mezer A, Wandell BA. The vertical occipital fasciculus: A century of controversy resolved by in vivo measurements. *Proc Natl Acad Sci USA* 2014; 111:E5214–E5223.
 161. Aydogan DB, Shi Y. Parallel transport tractography. *IEEE Trans Med Imaging* 2021; 40:635–647.
 162. Takemura H, Palomero-Gallagher N, Axer M, et al. Anatomy of nerve fiber bundles at micrometer-resolution in the vervet monkey visual system. *eLife* 2020; 9:e55444.
 163. Li K, Lu C, Huang Y, Yuan L, Zeng D, Wu K. Alteration of fractional anisotropy and mean diffusivity in glaucoma: Novel results of a meta-analysis of diffusion tensor imaging studies. *PLoS One* 2014; 9:e97445.
 164. You Y, Joseph C, Wang C, et al. Demyelination precedes axonal loss in the transneuronal spread of human neurodegenerative disease. *Brain* 2019; 142:426–442.
 165. Kaushik M, Graham SL, Wang C, Klistorner A. A topographical relationship between visual field defects and optic radiation changes in glaucoma. *Invest Ophthalmol Vis Sci* 2014; 55:5770–5775.
 166. Kruper J, Richie-Halford A, Benson NC, et al. Convolutional neural network-based classification of glaucoma using optic radiation tissue properties. *Commun Med (Lond)* 2024; 4:72.
 167. Ohno N, Murai H, Suzuki Y, et al. Alteration of the optic radiations using diffusion-tensor MRI in patients with retinitis pigmentosa. *Br J Ophthalmol* 2015; 99:1051–1054.
 168. Duan Y, Norcia AM, Yeatman JD, Mezer A. The structural properties of major white matter tracts in strabismic amblyopia. *Invest Ophthalmol Vis Sci* 2015; 56:5152–5160.
 169. Henschen SE. On the visual path and centre. *Brain* 1893; 16:170–180.
 170. Inouye T. Die sehstroungen bei schussverletzungen der kortikalen sehspahre. Leipzig:W. Engelmann, 1909.
 171. Holmes G, Lister WT. Disturbances of vision from cerebral lesions, with special reference to the cortical representation of the macula. *Brain* 1916; 39:34–73.
 172. Wandell BA, Winawer J. Imaging retinotopic maps in the human brain. *Vision Res* 2011; 51:718–737.
 173. Ebeling U, Reulen HJ. Neurosurgical topography of the optic radiation in the temporal lobe. *Acta Neurochir (Wien)* 1988; 92:29–36.
 174. Benson NC, Butt OH, Datta R, Radoeva PD, Brainard DH, Aguirre GK. The retinotopic organization of striate cortex is well predicted by surface topology. *Curr Biol* 2012; 22:2081–2085.
 175. Benson NC, Butt OH, Brainard DH, Aguirre GK. Correction of distortion in flattened representations of the cortical surface allows prediction of V1-V3 functional organization from anatomy. *PLOS Comput Biol* 2014; 10:e1003538.
 176. Benson NC, Winawer J. Bayesian analysis of retinotopic maps. *eLife* 2018; 7:e40224.
 177. Kruper J, Benson NC, Caffarra S, et al. Optic radiations representing different eccentricities age differently. *Hum Brain Mapp* 2023; 44:3123–3135.
 178. Nelson SB, LeVay S. Topographic organization of the optic radiation of the cat. *J Comp Neurol* 1985; 240:322–330.
 179. Takemura MY, Hori M, Yokoyama K, et al. Alterations of the optic pathway between unilateral and bilateral optic nerve damage in multiple sclerosis as revealed by the combined use of advanced diffusion kurtosis imaging and visual evoked potentials. *Magn Reson Imaging* 2017; 39:24–30.
 180. Berman S, Backner Y, Krupnik R, et al. Conduction delays in the visual pathways of progressive multiple sclerosis patients covary with brain structure. *Neuroimage* 2020; 221:117204.
 181. Takemura H, Yuasa K, Amano K. Predicting neural response latency of the human early visual cortex from MRI-based tissue measurements of the optic radiation. *eNeuro* 2020; 7:ENEURO.0545-19.2020.
 182. Caffarra S, Joo SJ, Bloom D, Kruper J, Rokem A, Yeatman JD. Development of the visual white matter pathways mediates development of electrophysiological responses in visual cortex. *Hum Brain Mapp* 2021; 42:5785–5797.
 183. Chan AYC, Chang DHF. Neural correlates of sensory eye dominance in human visual white matter tracts. *eNeuro* 2022; 9:ENEURO.0232-22.2022.
 184. Minami S, Oishi H, Takemura H, Amano K. Inter-individual differences in occipital alpha oscillations correlate with white matter tissue properties of the optic radiation. *eNeuro* 2020; 7:ENEURO.0224-19.2020.
 185. Caffarra S, Kanopka K, Kruper J, et al. Development of the alpha rhythm is linked to visual white matter pathways and visual detection performance. *J Neurosci* 2024; 44:e0684232023.
 186. Webb CE, Viera Perez PM, Hoagey DA, Gonen C, Rodrigue KM, Kennedy KM. Age-related degradation of optic

- radiation white matter predicts visual, but not verbal executive functions. *Apert Neuro* 2022; 2:1–10.
187. Clarke S, Miklossy J. Occipital cortex in man: Organization of callosal connections, related myelo- and cytoarchitecture, and putative boundaries of functional visual areas. *J Comp Neurol* 1990; 298:188–214.
 188. Kennedy H, Dehay C, Bullier J. Organization of the callosal connections of visual areas V1 and V2 in the macaque monkey. *J Comp Neurol* 1986; 247:398–415.
 189. Van Essen DC, Newsome WT, Bixby JL. The pattern of interhemispheric connections and its relationship to extrastriate visual areas in the macaque monkey. *J Neurosci* 1982; 2:265–283.
 190. Dejerine J. Contribution à l'étude anatomopathologique et clinique des différents variétés de cécité verbale. Mémoires de la Société de Biologie 1892; 4:61–90.
 191. Binder JR, Mohr JP. The topography of callosal reading pathways. A case-control analysis. *Brain* 1992; 115:1807–1826.
 192. Caspers S, Axer M, Caspers J, et al. Target sites for transcallosal fibers in human visual cortex - A combined diffusion and polarized light imaging study. *Cortex* 2015; 72:40–53.
 193. Dougherty RF, Ben-Shachar M, Bammer R, Brewer AA, Wandell BA. Functional organization of human occipital-callosal fiber tracts. *Proc Natl Acad Sci USA* 2005; 102:7350–7355.
 194. Wakana S, Caprihan A, Panzenboeck MM, et al. Reproducibility of quantitative tractography methods applied to cerebral white matter. *Neuroimage* 2007; 36:630–644.
 195. Scherf KS, Thomas C, Doyle J, Behrmann M. Emerging structure-function relations in the developing face processing system. *Cereb Cortex* 2014; 24:2964–2980.
 196. Hynd GW, Hall J, Novey ES, et al. Dyslexia and corpus callosum morphology. *Arch Neurol* 1995; 52:32–38.
 197. von Plessen K, Lundervold A, Duta N, et al. Less developed corpus callosum in dyslexic subjects—a structural MRI study. *Neuropsychologia* 2002; 40:1035–1044.
 198. Ben-Shachar M, Dougherty RF, Wandell BA. White matter pathways in reading. *Curr Opin Neurobiol* 2007; 17:258–270.
 199. Dougherty RF, Ben-Shachar M, Deutsch GK, Hernandez A, Fox GR, Wandell BA. Temporal-callosal pathway diffusivity predicts phonological skills in children. *Proc Natl Acad Sci USA* 2007; 104:8556–8561.
 200. Frye RE, Hasan K, Xue L, et al. Splenium microstructure is related to two dimensions of reading skill. *Neuroreport* 2008; 19:1627–1631.
 201. Odegard TN, Farris EA, Ring J, McColl R, Black J. Brain connectivity in non-reading impaired children and children diagnosed with developmental dyslexia. *Neuropsychologia* 2009; 47:1972–1977.
 202. Huber E, Henriques RN, Owen JP, Rokem A, Yeatman JD. Applying microstructural models to understand the role of white matter in cognitive development. *Dev Cogn Neurosci* 2019; 36:100624.
 203. Genç E, Bergmann J, Singer W, Kohler A. Interhemispheric connections shape subjective experience of bistable motion. *Curr Biol* 2011; 21:1494–1499.
 204. Horowitz A, Barazany D, Tavor I, Bernstein M, Yovel G, Assaf Y. In vivo correlation between axon diameter and conduction velocity in the human brain. *Brain Struct Funct* 2015; 220:1777–1788.
 205. Berman S, Filo S, Mezer AA. Modeling conduction delays in the corpus callosum using MRI-measured g-ratio. *Neuroimage* 2019; 195:128–139.
 206. Boucard CC, Hanekamp S, Čurčić-Blake B, Ida M, Yoshida M, Cornelissen FW. Neurodegeneration beyond the primary visual pathways in a population with a high incidence of normal-pressure glaucoma. *Ophthalmic Physiol Opt* 2016; 36:344–353.
 207. Takemura H, Rokem A, Winawer J, Yeatman JD, Wandell BA, Pestilli F. A major human white-matter pathway between dorsal and ventral visual cortex. *Cereb Cortex* 2016; 26:2205–2214.
 208. Yeatman JD, Rauschecker AM, Wandell BA. Anatomy of the visual word form area: Adjacent cortical circuits and long-range white matter connections. *Brain Lang* 2013; 125:146–155.
 209. Martino J, Garcia-Porrero JA. In Reply: Wernicke perpendicular fasciculus and vertical portion of the superior longitudinal fasciculus. *Neurosurgery* 2013; 73:E382–E383.
 210. Wu Y, Sun D, Wang Y, Wang Y, Wang Y. Tracing short connections of the temporo-parieto-occipital region in the human brain using diffusion spectrum imaging and fiber dissection. *Brain Res* 2016; 1646:152–159.
 211. Jitsuishi T, Hirono S, Yamamoto T, Kitajo K, Iwadate Y, Yamaguchi A. White matter dissection and structural connectivity of the human vertical occipital fasciculus to link vision-associated brain cortex. *Sci Rep* 2020; 10:820.
 212. Takemura H, Pestilli F, Weiner KS, et al. Occipital white matter tracts in human and macaque. *Cereb Cortex* 2017; 27:3346–3359.
 213. Ungerleider LG, Mishkin M. Two cortical visual systems, In: Ingle DJ Goodale MA Mansfield RJW eds. The analysis of visual behavior. Cambridge:MIT Press 1982: 549–586.
 214. Goodale MA, Milner AD. Separate visual pathways for perception and action. *Trends Neurosci* 1992; 15:20–25.
 215. Greenblatt SH. Alexia without agraphia or hemianopsia. Anatomical analysis of an autopsied case. *Brain* 1973; 96:307–316.
 216. Kay KN, Yeatman JD. Bottom-up and top-down computations in word- and face-selective cortex. *eLife* 2017; 6:e22341.
 217. Schurr R, Filo S, Mezer AA. Tractography delineation of the vertical occipital fasciculus using quantitative T1 mapping. *Neuroimage* 2019; 202:116121.
 218. Oishi H, Takemura H, Aoki SC, Fujita I, Amano K. Microstructural properties of the vertical occipital fasciculus explain the variability in human stereoacuity. *Proc Natl Acad Sci USA* 2018; 115:12289–12294.
 219. Murphy AP, Leopold DA, Humphreys GW, Welchman AE. Lesions to right posterior parietal cortex impair visual depth perception from disparity but not motion cues. *Philos Trans R Soc Lond B Biol Sci* 2016; 371: 20150263.
 220. Abdolalizadeh A, Mohammadi S, Aarabi MH. The forgotten tract of vision in multiple sclerosis: Vertical occipital

- fasciculus, its fiber properties, and visuospatial memory. *Brain Struct Funct* 2022; 227:1479–1490.
221. Broce IJ, Bernal B, Altman N, et al. Fiber pathways supporting early literacy development in 5–8-year-old children. *Brain Cogn* 2019; 134:80–89.
 222. Forkel SJ, Labache L, Nachev P, Thiebaut de Schotten M, Hesling I. Stroke disconnectome decodes reading networks. *Brain Struct Funct* 2022; 227:2897–2908.
 223. Grotheer M, Yeatman J, Grill-Spector K. White matter fascicles and cortical microstructure predict reading-related responses in human ventral temporal cortex. *Neuroimage* 2021; 227:117669.
 224. Lerma-Usabiaga G, Carreiras M, Paz-Alonso PM. Converging evidence for functional and structural segregation within the left ventral occipitotemporal cortex in reading. *Proc Natl Acad Sci USA* 2018; 115:E9981–E9990.
 225. Zilles K, Palomero-Gallagher N, Gräßel D, et al. Chapter 18 - High-resolution fiber and fiber tract imaging using polarized light microscopy in the human, monkey, rat, and mouse brain, In: Rockland KS ed. Axons and brain architecture. Academic Press, 2016; 369–389.
 226. Caspers S, Axer M. Decoding the microstructural correlate of diffusion MRI. *NMR Biomed* 2019; 32:e3779.
 227. Lanciego JL, Wouterlood FG. Neuroanatomical tract-tracing techniques that did go viral. *Brain Struct Funct* 2020; 225:1193–1224.
 228. Rockland KS. What we can learn from the complex architecture of single axons. *Brain Struct Funct* 2020; 225:1327–1347.
 229. Jones R, Grisot G, Augustinack J, et al. Insight into the fundamental trade-offs of diffusion MRI from polarization-sensitive optical coherence tomography in ex vivo human brain. *Neuroimage* 2020; 214:116704.
 230. Caspers S, Axer M, Gräßel D, Amunts K. Additional fiber orientations in the sagittal stratum-noise or anatomical fine structure?. *Brain Struct Funct* 2022; 227:1331–1345.
 231. Kiryu-Seo S, Matsushita R, Tashiro Y, et al. Impaired disassembly of the axon initial segment restricts mitochondrial entry into damaged axons. *EMBO J* 2022; 41:e110486.
 232. Beaulieu C, Does MD, Snyder RE, Allen PS. Changes in water diffusion due to Wallerian degeneration in peripheral nerve. *Magn Reson Med* 1996; 36:627–631.
 233. Henriques RN, Correia MM, Marrale M, et al. Diffusional kurtosis imaging in the diffusion imaging in python project. *Front Hum Neurosci* 2021; 15:675433.
 234. Vollmar C, O’Muircheartaigh J, Barker GJ, et al. Identical, but not the same: Intra-site and inter-site reproducibility of fractional anisotropy measures on two 3.0T scanners. *Neuroimage* 2010; 51:1384–1394.
 235. Grech-Sollars M, Hales PW, Miyazaki K, et al. Multi-centre reproducibility of diffusion MRI parameters for clinical sequences in the brain. *NMR Biomed* 2015; 28:468–485.
 236. Han X, Jovicich J, Salat D, et al. Reliability of MRI-derived measurements of human cerebral cortical thickness: The effects of field strength, scanner upgrade and manufacturer. *Neuroimage* 2006; 32:180–194.
 237. Yan C-G, Craddock RC, Zuo X-N, Zang Y-F, Milham MP. Standardizing the intrinsic brain: Towards robust measurement of inter-individual variation in 1000 functional connectomes. *Neuroimage* 2013; 80:246–262.
 238. Wang Y-W, Chen X, Yan C-G. Comprehensive evaluation of harmonization on functional brain imaging for multisite data-fusion. *Neuroimage* 2023; 274:120089.
 239. Cetin Karayumak S, Bouix S, Ning L, et al. Retrospective harmonization of multi-site diffusion MRI data acquired with different acquisition parameters. *Neuroimage* 2019; 184:180–200.
 240. Ning L, Bonet-Carne E, Grussu F, et al. Cross-scanner and cross-protocol multi-shell diffusion MRI data harmonization: Algorithms and results. *Neuroimage* 2020; 221:117128.
 241. Kurokawa R, Kamiya K, Koike S, et al. Cross-scanner reproducibility and harmonization of a diffusion MRI structural brain network: A traveling subject study of multi-b acquisition. *Neuroimage* 2021; 245:118675.
 242. Moyer D, Ver Steeg G, Tax CMW, Thompson PM. Scanner invariant representations for diffusion MRI harmonization. *Magn Reson Med* 2020; 84:2174–2189.
 243. Pinto MS, Paoletta R, Billiet T, et al. Harmonization of brain diffusion MRI: Concepts and methods. *Front Neurosci* 2020; 14:396.
 244. Lerma-Usabiaga G, Mukherjee P, Ren Z, Perry ML, Wandell BA. Replication and generalization in applied neuroimaging. *Neuroimage* 2019; 202:116048.
 245. Weiskopf N, Mohammadi S, Lutti A, Callaghan MF. Advances in MRI-based computational neuroanatomy: From morphometry to in-vivo histology. *Curr Opin Neurol* 2015; 28:313–322.
 246. Cercignani M, Dowell NG, Tofts PS. Quantitative MRI of the brain: Principles of physical measurement, second edition. Boca Raton: CRC Press, 2018
 247. Richie-Halford A, Yeatman JD, Simon N, Rokem A. Multidimensional analysis and detection of informative features in human brain white matter. *PLOS Comput Biol* 2021; 17:e1009136.
 248. Chamberland M, Genc S, Tax CMW, et al. Detecting microstructural deviations in individuals with deep diffusion MRI tractometry. *Nat Comput Sci* 2021; 1:598–606.
 249. Rokem A, Qiao J, Yeatman JD, Richie-Halford A. Incremental improvements in tractometry-based brain-age modeling with deep learning. *bioRxiv* 2023.03.02.530885.
 250. Van Essen DC, Smith SM, Barch DM, Behrens TE, Yacoub E, Ugurbil K. The WU-Minn Human Connectome Project: An overview. *Neuroimage* 2013; 80:62–79.
 251. Glasser MF, Smith SM, Marcus DS, et al. The Human Connectome Project’s neuroimaging approach. *Nat Neurosci* 2016; 19:1175–1187.
 252. Alexander LM, Escalera J, Ai L, et al. An open resource for transdiagnostic research in pediatric mental health and learning disorders. *Sci Data* 2017; 4:170181.
 253. Richie-Halford A, Cieslak M, Ai L, et al. An analysis-ready and quality controlled resource for pediatric brain white-matter research. *Sci Data* 2022; 9:616.
 254. Jernigan TL, Brown SA, Dowling GJ. The adolescent brain cognitive development study. *J Res Adolesc* 2018; 28:154–156.

255. Sudlow C, Gallacher J, Allen N, et al. UK biobank: An open access resource for identifying the causes of a wide range of complex diseases of middle and old age. *PLoS Med* 2015; 12: e1001779.
256. Bastiani M, Andersson JLR, Cordero-Grande L, et al. Automated processing pipeline for neonatal diffusion MRI in the developing Human Connectome Project. *Neuroimage* 2019; 185:750–763.
257. Koike S, Tanaka SC, Okada T, et al. Brain/MINDS beyond human brain MRI project: A protocol for multi-level harmonization across brain disorders throughout the lifespan. *Neuroimage Clin* 2021; 30:102600.
258. Marek S, Tervo-Clemmens B, Calabro FJ, et al. Reproducible brain-wide association studies require thousands of individuals. *Nature* 2022; 603:654–660.
259. Gratton C, Nelson SM, Gordon EM. Brain-behavior correlations: Two paths toward reliability. *Neuron* 2022; 110:1446–1449.
260. Smith PL, Little DR. Small is beautiful: In defense of the small-N design. *Psychon Bull Rev* 2018; 25:2083–2101.
261. Naselaris T, Allen E, Kay K. Extensive sampling for complete models of individual brains. *Curr Opin Behav Sci* 2021; 40:45–51.
262. Puzniak RJ, McPherson B, Ahmadi K, et al. CHIASM, the human brain albinism and achiasma MRI dataset. *Sci Data* 2021; 8:308.
263. Heilbronner SR, Haber SN. Frontal cortical and subcortical projections provide a basis for segmenting the cingulum bundle: Implications for neuroimaging and psychiatric disorders. *J Neurosci* 2014; 34:10041–10054.
264. Muncy NM, Kimbler A, Hedges-Muncy AM, McMakin DL, Mattfeld AT. General additive models address statistical issues in diffusion MRI: An example with clinically anxious adolescents. *Neuroimage Clin* 2022; 33:102937.
265. Huang S-H, Li M-J, Yeh F-C, Huang C-X, Zhang H-T, Liu J. Differential and correlational tractography as tract-based biomarkers in mild traumatic brain injury: A longitudinal MRI study. *NMR Biomed* 2023; 36:e4991.
266. Wickham H. Tidy Data. *J Stat Softw* 2014; 59:1–23.
267. Yeatman JD, Richie-Halford A, Smith JK, Keshavan A, Rokem A. A browser-based tool for visualization and analysis of diffusion MRI data. *Nat Commun* 2018; 9:940.
268. Tapera TM, Cieslak M, Bertolero M, et al. FlywheelTools: Data curation and manipulation on the Flywheel platform. *Front Neuroinform* 2021; 15:678403.
269. Renton AI, Dao TT, Johnstone T, et al. Neurodesk: An accessible, flexible and portable data analysis environment for reproducible neuroimaging. *Nat Methods* 2024; 21:804–808.
270. Hayashi S, Caron BA, Heinsfeld AS, et al. brainlife.io: A decentralized and open-source cloud platform to support neuroscience research. *Nat Methods* 2024; 21:809–813.
271. Grotheer M, Kubota E, Grill-Spector K. Establishing the functional relevancy of white matter connections in the visual system and beyond. *Brain Struct Funct* 2022; 227:1347–1356.
272. Thiebaut de Schotten M, Crosson PL, Mars RB. Large-scale comparative neuroimaging: Where are we and what do we need? *Cortex* 2019; 118:188–202.
273. Takemura H, Pestilli F, Weiner KS. Comparative neuroanatomy: Integrating classic and modern methods to understand association fibers connecting dorsal and ventral visual cortex. *Neurosci Res* 2019; 146:1–12.
274. Kaneko T, Takemura H, Pestilli F, Silva AC, Ye FQ, Leopold DA. Spatial organization of occipital white matter tracts in the common marmoset. *Brain Struct Funct* 2020; 225:1313–1326.
275. López-Elizalde R, Godínez-Rubí M, Lemus-Rodríguez Y, et al. Anatomy of the optic nerve based on cadaveric dissections and its neurosurgical approaches: A comprehensive review. *Sechenov Med J* 2021; 12:5–18.
276. Tzourio-Mazoyer N, Landeau B, Papathanassiou D, et al. Automated anatomical labeling of activations in SPM using a macroscopic anatomical parcellation of the MNI MRI single-subject brain. *Neuroimage* 2002; 15:273–289.